

**Nurturing the Blossoming Hydrogen Economy Using HBAT:  
Modelling Every Link in the H<sub>2</sub> Supply Chain**

Journal:	<i>Energy &amp; Environmental Science</i>
Manuscript ID	EE-ANA-08-2023-002789.R1
Article Type:	Analysis
Date Submitted by the Author:	27-Nov-2023
Complete List of Authors:	Alfonso Vargas, Nicolas; University of Southern California, Chemistry Kim, Moon Jung; University of Southern California, Chemical Biology Alfonso, Daniel; University of South Florida Alfonso Vargas, Carlos; University of Central Florida Evans, Justin; University of Central Florida

**Broader Context Statement:**

Scaling sustainable energy relies on intermittent power generators like wind and solar, which need to generate surplus electricity to meet the full day's demand. Currently, excess variable renewable energy (VRE) is often curtailed or stored in site-specific facilities such as pumped hydro. However, a more flexible approach involves storing the excess VRE within energy-dense molecules that can be easily transported. Hydrogen and hydrogen carriers serve as such molecules and can be transported via various means e.g., truck, railcar, barge, or pipeline. Hydrogen gas is notoriously difficult to handle, given its permeability through steel, high flammability, and high molecular volume. Evaluating the economic viability of different hydrogen forms (gas, liquid, or carried) is key to this strategy. The Hydrogen Business Appraisal Tool (HBAT) provides valuable financial, environmental, and societal insights into user-defined combinations of hydrogen supply chains. By showcasing 64 supply chain combinations, this analysis serves to calibrate understanding and shed light on the economic potential and trajectory of the developing hydrogen economy. Figure 1 demonstrates how supply chain **17** is studied in this analysis.

## ARTICLE

## Nurturing the Blossoming Hydrogen Economy Using HBAT: Modelling Every Link in the H<sub>2</sub> Supply Chain

Nicolas Alfonso Vargas,<sup>a,§</sup> Moon Jung Kim,<sup>b,§</sup> Carlos D. Alfonso Vargas<sup>c</sup>, Daniel F. Alfonso,<sup>d</sup> and Justin T. Evans<sup>c</sup>

Received 00th January 20xx,  
Accepted 00th January 20xx

DOI: 10.1039/x0xx00000x

An exclusively renewable energy economy is imperative for sustained industrial expansion. Despite notable progress, renewable energy sources fulfilled only 12.6% of global energy demand in 2022. This can be largely attributed to the suboptimal capacity utilisation of most renewable energy generators. Addressing this challenge, hydrogen and liquid organic hydrogen carriers (LOHCs) offer a distinct solution by leveraging economies of scale to substantially lower the levelised costs of delivery beyond current U.S. D.o.E. targets. While several techno-economic assessments have examined specific hydrogen technologies, none have comprehensively evaluated numerous supply chain variations with consistent and comparable assumptions. Showcasing the Hydrogen Business Appraisal Tool (HBAT), we present a techno-economic analysis that evaluates technologies for the entire hydrogen supply chain, incorporating economic, environmental, and societal considerations for 64 unique variations. Notably, our study reveals efficient production capacities for each supply chain combination, suggests optimal reinvestment strategies, and quantifies the economic impact of continued investment in R&D for technology efficiency and longevity. Moreover, our analysis uncovers the environmental hazards associated with various hydrogen storage media, providing critical insights for sustainability decision-making.

### Broader Context

Scaling sustainable energy relies on intermittent power generators like wind and solar, which need to generate surplus electricity to meet the full day's demand. Currently, excess variable renewable energy (VRE) is often curtailed or stored in site-specific facilities such as pumped hydro. However, a more flexible approach involves storing the excess VRE within energy-dense molecules that can be easily transported. Hydrogen and hydrogen carriers serve as such molecules and can be transported via various means e.g., truck, railcar, barge, or pipeline. Hydrogen gas is notoriously difficult to handle, given its permeability through steel, high flammability, and high molecular volume. Evaluating the economic viability of different hydrogen forms (gas, liquid, or carried) is key to this strategy. The Hydrogen Business Appraisal Tool (HBAT) provides valuable financial, environmental, and societal insights into user-defined combinations of hydrogen supply chains. By showcasing 64 supply chain combinations, this analysis serves to calibrate understanding and shed light on the economic potential and trajectory of the developing hydrogen economy. Figure 1 demonstrates how supply chain 17 is studied in this analysis.

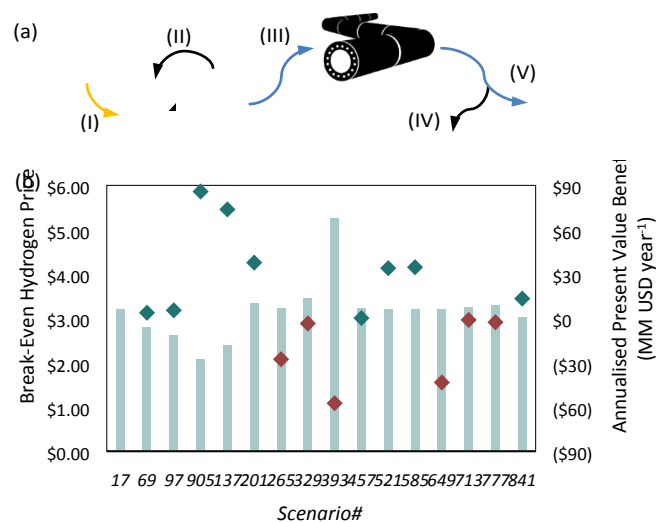


**Fig. 1** Supply chain 17 modelled in HBAT. (a) Initial investment in 2025 includes 274 MW photo-voltaic arrays coupled to CO<sub>2</sub> electrolysers producing 695 tonnes of CO per day. Formic acid is manufactured from the CO and water using catalytic methanol and delivered by pipeline followed by dehydrogenation to ammonia manufacturers surrounding Chambers County in Texas, USA. (I) Electricity from renewable or sustainable sources; (II) CO<sub>2</sub> extracted from manufacturing waste streams; (III) Formic acid produced from the carbonylation of methanol and subsequent ester hydrolysis; (IV) CO<sub>2</sub> waste; (V) H<sub>2</sub> delivered for ammonia manufacturing. (b) Break-Even Hydrogen Price (BEHP) for all supply chain 17 scenarios as bars, plotted with the annualised present value benefit or (cost) of each variation as diamonds. Scenario 17 is the default scenario of which all other scenarios are compared to.

<sup>a</sup> Department of Chemistry, University of Southern California, Los Angeles, CA 90007, USA. Corresponding author. Email: nalfonso@usc.edu

<sup>b</sup> Department of Chemistry, University of Southern California, Los Angeles, CA 90007, USA. Email: moonjung@usc.edu

<sup>c</sup> University of Central Florida, Orlando, FL 32816, USA

<sup>d</sup> University of South Florida, Tampa, FL 33620, USA

<sup>§</sup> Co-first authors with equal contributions.

Electronic Supplementary Information (ESI) available: SI-data table.xlsx; Supplemental Information.docx. See DOI: 10.1039/x0xx00000x

**Table of Contents**

Section 0: <b>Broader Context</b>	Fig. 1 - <b>p. 1</b>
Section 1: <b>Introduction</b>	<b>p. 3</b>
Section 2: <b>Methods</b>	<b>p. 3 – 12</b>
Section 2.1: Technologies – Production	Table 1; Fig. 2 & 3 - <b>p. 4</b>
Section 2.2: Technologies – Storage	Fig. 4; Scheme 1 & 2 - <b>p. 5</b>
Section 2.3: Technologies – Transportation	Equations 1 – 6 - <b>p. 8</b>
Section 2.4: Technologies – End-use	Fig. 5 & 6 - <b>p. 9</b>
Section 2.5: Scenarios	Table 2; Fig. 7 - <b>p. 9</b>
Section 2.6: Economic model	Equations 7 – 35 - <b>p. 11</b>
Section 2.7: Environmental model	<b>p. 12</b>
Section 3: <b>Results and Discussion</b>	<b>p. 12 – 26</b>
Section 3.1: Supply chain screening	Fig. 8 & 9 – <b>p. 12</b>
Section 3.2: Profitability and levelised cost analysis	Equation 36; Fig. 10 – 13 - <b>p. 13</b>
Section 3.3: Installed capacity analysis	Table 3; Fig. 14– 16 - <b>p. 15</b>
Section 3.4: Electrolyser longevity analysis	Fig. 17 – 18 - <b>p. 18</b>
Section 3.5: Electrolyser utilisation optimisation	Fig. 19 – 21 - <b>p. 18</b>
Section 3.6: Cost-reduction analysis	Equations 37 – 39; Fig. 22 – 25 - <b>p. 20</b>
Section 3.7: Environmental impact	Table 4; Fig. 26 – 30 - <b>p. 22</b>
Section 3.8: Societal impact	Fig. 31 & 32 - <b>p. 25</b>
Section 4: <b>Summary and Conclusions</b>	<b>p. 26 – 28</b>
Section 5: <b>References</b>	<b>p. 28 – 30</b>

## 1 Introduction

Given the growing concern for climate change and increasing support for environmental and social accountability, variable renewable energy (VRE) growth is projected to accelerate significantly over the next 25 years.<sup>1</sup> In order to match the growing VRE supply, it is essential to boost efficiency, decrease capital costs, and increase investments in VRE infrastructure. Despite recent technological advances and reduced capital costs leading to record expansions of renewable electricity capacity,<sup>2</sup> public and private institutions are still reluctant to rely on utility-scale VRE. A 2021 NREL study<sup>3</sup> found that as the share of VRE grows, curtailment increases thus eliminating the economies-of-scale benefit and un-incentivizing the expansion of VRE facilities. Institutions worry this could lead to power outages and losses in revenue if traditional power plants do not supplement the supply. To overcome this counterproductive cycle, solutions for storing excess VRE must be developed.

Wind and solar account for 64% of the U.S. renewable energy mix<sup>4</sup> and will be responsible for 65% of additional utility-scale capacity in 2023. While these sources have greatly contributed to decarbonisation efforts across various sectors, they suffer from major limitations that prevent large-scale deployment of these technologies – namely energy storage and dispatchability. Because wind and solar are intermittent energy sources, affordable high-capacity energy storage methods must be established to minimise power fluctuations and maintain the delivery of on-demand power in a reliable and economical manner. Current state-of-the-art energy storage technologies include lithium-ion batteries,<sup>5</sup> pumped storage hydropower (PSH),<sup>6</sup> and compressed air energy storage (CAES)<sup>7</sup> among others.<sup>8</sup> While these technologies are generally reliable and excel in local, short-term energy storage, the energy storage and delivery capacity needed to eliminate VRE curtailment is economically unattainable. In addition to this, wind turbines and solar farms are strategically sited in geographic locations where the environment and latitude are favourable for harnessing the full potential of wind and solar power. However, these locations typically remain remote and are located at great distances from major cities and industries where energy demand is high. Even with the existing electric transmission infrastructure, electrical energy can only be dispatched throughout a defined region in proximity to the power generator. Given these limitations, there is a clear need for an alternative solution that addresses the issue of storing and dispatching excess VRE and eliminating curtailment completely.

Hydrogen and energy have a long-shared history. Government support for hydrogen R&D dates back to the 1970s.<sup>9</sup> Hydrogen piqued the interest of many scientists and engineers because of its physical and chemical properties that lend itself to being an excellent energy carrier. Among the existing combustibles, hydrogen has the highest energy density – over 2.5-fold greater than the next highest energy-dense molecule, methane. In addition to being energy dense, hydrogen is extremely light, storable, and produces zero direct greenhouse gas emissions. This makes hydrogen both economically and environmentally

feasible as a means of storing and delivering tremendous amounts of energy. Many technologies for hydrogen production, storage, and transport are readily available to enable the use of hydrogen in different ways. Hydrogen can be produced from a variety of sources including renewables,<sup>10</sup> nuclear,<sup>11</sup> coal,<sup>12</sup> natural gas,<sup>13</sup> and depleted oil wells.<sup>14</sup> It can be transported in gaseous form by pipelines or as a cryogenic liquid<sup>15</sup> by trucks and barge. Furthermore, hydrogen can be used for heating, generating electricity, and as a feedstock for various industrial processes such as petroleum refining<sup>16</sup> and fertiliser manufacturing.<sup>17</sup> For these reasons, hydrogen is extremely versatile and can be used to accelerate decarbonisation across a range of sectors where reducing emissions is difficult. As of the end of 2022, the global demand for hydrogen is 95 MMT<sup>18</sup> annually with some projecting a 4- to 6-fold increase in demand by 2050.<sup>19</sup> To meet the current demand, hydrogen is typically produced at industrial scales on-site and almost entirely from fossil fuels – accounting for 4% of global natural gas consumption and resulting in 900 MMT of annual CO<sub>2</sub> emissions. In order to transition towards a clean energy future, CO<sub>2</sub> capture technologies along with green hydrogen production methods must be employed. However, the cost of producing hydrogen from clean electricity is significantly higher than hydrogen produced from fossil fuels, imposing a major barrier in its role in a clean energy future. Storing inexpensive and abundant sources of clean energy for producing hydrogen is crucial for providing green hydrogen at a reduced cost – approaching the DOE Hydrogen Shot goal of \$1 per 1 kg in 1 decade.<sup>20</sup>

## 2 Methods

The Hydrogen Business Appraisal Tool (HBAT)<sup>21</sup> is a comprehensive automated business modelling tool that provides users with insights into the financial, environmental, and societal properties of up to 1092 different supply chains across 8 locations involved in the production and distribution of hydrogen. In this study, we modelled a set of 64 relevant supply chains while varying six financial parameters individually to generate 824 distinct business case scenarios. Within each scenario, HBAT populates an equipment expense list to calculate the Total Installed Cost ( $C_{TI}$ ) and Total Plant Cost ( $C_{TP}$ ). Using default or user-defined financial assumptions such as equipment depreciation rates, cost scaling factors, and future cost reductions, HBAT then provides the user with a complete CAPEX summary, OPEX summary, and Cash Flow Analysis for the user-selected timeframe. Additionally, an environmental impact report is given to inform the user of how their selected scenario benefits or diminishes environmental health. This includes the intrinsic carbon footprint, organic and inorganic pollutant emissions, and inventory toxicity. From these analyses, we compiled key financial and environmental information for each scenario to determine its economic potential and environmental impact. Additionally, HBAT's unique societal analysis combines poll data and employment numbers to report socioeconomic statistics. The following sections describe how HBAT processes the data collected.

Production Pathway	Data Source
H <sub>2</sub> O Electrolysis	H2A model <sup>22</sup>
PV-Coupled H <sub>2</sub> O Electrolysis	H2A model <sup>22</sup> , Feldman et al. <sup>23</sup>
CO <sub>2</sub> Electrolysis	Lee et al. <sup>24</sup>
PV-Coupled CO <sub>2</sub> Electrolysis	Lee et al. <sup>24</sup> , Feldman et al. <sup>23</sup>
Electrochemical N <sub>2</sub> Reduction	Gomez et al. <sup>25</sup> , Cha et al. <sup>26</sup>
PV-Coupled N <sub>2</sub> Reduction	Gomez et al. <sup>25</sup> , Feldman et al. <sup>23</sup>
Steam Methane Reforming	Byun et al. <sup>27</sup>
SMR to Methanol	Labbaef et al. <sup>28</sup>
Wood Biomass Gasification	Salkuyeh et al. <sup>29</sup>
CO Water Gas Shift	Kramer <sup>30</sup>
Chlor-Alkali Process	Lee et al. <sup>31</sup>

**Table 1** Hydrogen production technologies and economic data source.

## 2.1 Technologies – Production

Despite the rising interest and development in hydrogen storage and transportation technologies, hydrogen production remains the primary influence on the economic viability of a given business case. HBAT is capable of modelling seven production technologies with the option to vary four additional parameters to generate eleven distinct production pathways. Table 1 lists these production pathways and the source of their economic data. While HBAT can model all these pathways, the following technologies were chosen to be used in this economic analysis.

### *H<sub>2</sub>O Electrolysis*

Water electrolyzers have existed for centuries, with the first technical application used in 1890 to produce hydrogen for French airships. The issue with using electrolyzers as a form of energy storage is the inherent resistance caused by current passing through heterogeneous phases. This relatively large resistance requires overpotentials that convert part of the supplied electrical energy into heat rather than productive chemical energy. The amount of energy required to split liquid water into 1 kg of hydrogen is equal to the higher heating value (HHV) of 39.41 kWh. According to discussions with manufacturing representatives, a PEM electrolyzer can typically achieve efficiencies between 49.9 and 41 kWh kg<sup>-1</sup>, skewed to the higher end of that range. Estimates were also provided for current uninstalled costs of state-of-the-art electrolyzers: 500 USD kW<sup>-1</sup> @1 GW and 600 USD kW<sup>-1</sup> @500 MW. Using a National Renewable Energy Laboratory (NREL) estimate<sup>22</sup> of the price of a 1 MW electrolyzer, a cost curve was created to estimate the current capital cost of water electrolyzers at varying scales, shown in Figure 2. These estimates include the deioniser and material costs, but do not include the balance-of-plant or installation cost. The default depreciation function for all electrolyzers in HBAT is a linear 10-year lifetime with no salvageable asset remaining. This can be changed manually, and such examples are shown in this report where the linear lifetime is changed to 20 and 40 years. Counter-intuitively, this does not mean to imply that the electrolyzer can operate for 20 or 40 years continuously. For example, halfway through the lifetime,

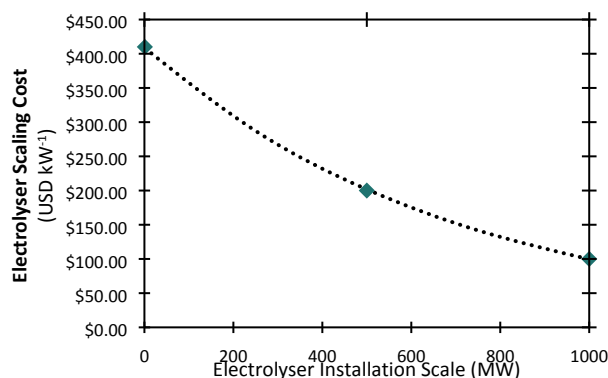


**Fig. 2** Electrolyzer Scaling Cost curve. Base Cost = \$400 kW<sup>-1</sup>. Electrolyzer Total Module Cost = Base Cost + Scaling Cost.

an investment equal to half the cost of the electrolyzer is made to maintain full operation. In these speculative cases where the electrolyzer lifetime is longer than the current state-of-the-art, the business case is studying how the economics change if R&D prioritises increasing the electrolyzer's longevity.

### *CO<sub>2</sub> Electrolysis*

Carbon dioxide electrolyzers are much less mature than that of their water counterparts. While water electrolysis has clear frontrunners for the most effective electrolyzer design, CO<sub>2</sub> electrolysis is a budding technology involving many different styles of electrochemical reduction. This umbrella term encompasses CO<sub>2</sub> reduction to carbon monoxide, methane, methanol, ethylene, ethanol, and many other reduction products. Each one of these products requires drastically different catalysts, membranes, and reaction conditions. The most mature of these electrochemical processes is the CO<sub>2</sub> reduction to CO. This is the reaction our CO<sub>2</sub> Electrolysis production pathway focuses on. Using the techno-economic analysis published in 2019 by Lee and co-workers<sup>24</sup> we gathered the cost and efficiency data necessary to integrate this production technology into the HBAT economic model. Carbon monoxide is a versatile molecule that can be used to simply reduce water to hydrogen using the water gas shift (WGS) reaction or can be converted to liquid organic hydrogen carrier (LOHC) molecules. These LOHC's can be stored and transported with minimal energy loss relative to hydrogen's natural phases.

### *Electrochemical N<sub>2</sub> Reduction*

Another budding technology soon to be commercialised is the electrochemical reduction of nitrogen for ammonia production. Countries such as Saudi Arabia have already invested billions of USD to create green ammonia production facilities. Green ammonia can be manufactured either by using green hydrogen in the well-established Haber-Bosch (HB) process or by electrochemically reducing nitrogen in the presence of hydrogen. To simplify the economic model, we selected the latter for the primary study due to findings by Gomez and co-workers<sup>25</sup> that it had the potential to have the lowest levelised cost of all green ammonia pathways. To maintain consistency, the efficiency data from water electrolyzers were used for this pathway, but all cost models were extracted from the Gomez

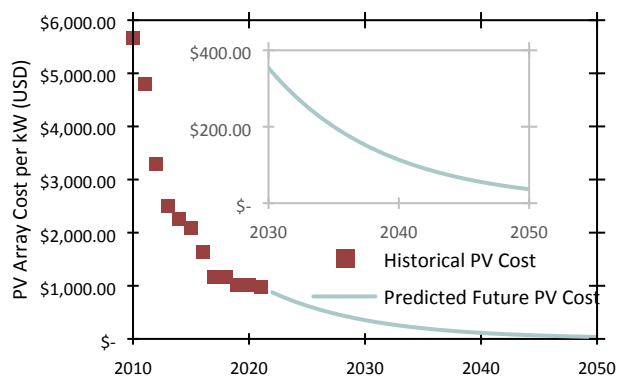


Fig. 3 Historical and predicted utility-scale PV array cost used in HBAT.

analysis. This production pathway is only used to transport ammonia; this study assumes no other hydrogen storage medium is compatible. The HB-coupled process is also evaluated for comparison in section 3.1.

#### Photo-Voltaic (PV) Coupling

Electrolysis business cases heavily depend on the electricity source. As described by NREL in their H2@Scale concept,<sup>32</sup> electricity for water electrolysis must cost less than 0.08 USD kWh<sup>-1</sup> to produce hydrogen at less than 4.50 USD kg<sup>-1</sup>, even with an optimistic electrolyser cost of 400 USD kW<sup>-1</sup>. For this reason, this analysis decided to set dedicated PV-coupled electrolysis as the standard to ensure that the electricity is renewable and available without relying on electricity demand functions. Costs for utility-scale PV arrays have steadily been dropping, providing an opportunity to invest in large installations that will decarbonise industry. Using a weighted average of the PV price reduction each year, and assigning higher weights to more recent years, the average annual price reduction was found to be 10.7%. This average is then extrapolated to 2050 and used to predict the PV module costs when built at different points in time as shown in Figure 3.

Due to the surface area requirement of utility-scale PV arrays, real estate investment strongly depends on the power generation capacity of the arrays. The amount of real-estate area required is calculated by assuming a surface power density of 182.9 W m<sup>-2</sup>.

#### Steam Methane Reforming

Natural gas is one of Earth's most abundant fuel resources. In locations where natural gas is affordable, steam methane reforming (SMR) is the most economical technique used to produce on-demand hydrogen. The natural gas consumption calculated by HBAT is based on the stoichiometric ratio between methane and the hydrogen produced from both SMR and water-gas shift (1:4 CH<sub>4</sub>:H<sub>2</sub>). The heat requirement is assumed to be fulfilled by renewably sourced electricity to minimise carbon emissions.

The SMR economics depend heavily on the variable operating costs. The price of the water, natural gas, and electricity consumed by the process typically dictates whether the business case is feasible. HBAT assumes a natural gas price of

6.50 USD MMBTU<sup>-1</sup>. However, future legislation, trade agreements, and supply have the potential to inflate the market price drastically. While it is difficult to predict what future prices may be, this report models how the economics will change at 9.00 and 11.50 USD MMBTU<sup>-1</sup> to understand its sensitivity.

#### Wood Biomass Gasification

One of the most anticipated upcoming technologies for mass manufacturing of hydrogen is wood biomass gasification. This pathway involves degrading wood excess such as stumps, shavings, and branches into syngas (H<sub>2</sub>/CO mix) using high-temperature steam and oxygen. This syngas can then be further modified by WGS to release additional hydrogen and carbon dioxide by-product. Many believe biomass gasification is a carbon neutral process because the feedstock's carbon is sourced from atmospheric carbon dioxide, i.e. biogenic. This is a fallacy because the biomass, or in this case wood, would always be converted back into carbon dioxide at a greater rate than the atmospheric carbon dioxide being sequestered by flora. Therefore, this study calculates the carbon footprint of all biomass gasification supply chains by including the total amount of carbon consumed by the process. There are other biomass gasification processes that use microbial biomass that has the potential to be carbon neutral, but these technologies were not found to be mature enough to include in this study.

The economics and energy data used to model this pathway was gathered from the Salkuyeh and co-workers' techno-economic analysis.<sup>29</sup> The authors studied several variations of pine-wood gasification processes and found the most economical to be a fluidised-bed gasifier without carbon-capture. HBAT uses this data along with their assumption for pine-wood price (100 USD tonne<sup>-1</sup>).

#### CO Purchase and Water-Gas Shift

Due to the increasing chemical value of carbon monoxide, HBAT includes a pathway that starts by purchasing crude CO in bulk from manufacturers that sell it as a by-product. This CO is then purified and can be used to make LOHC's or hydrogen by WGS. Due to the simplicity of this pathway, the economics rely almost entirely on the CO price, by default set at 600 USD tonne<sup>-1</sup>. The WGS process economics data were gathered from the Gas Technology Institute Final Technical Report by Kramer.<sup>30</sup>

## 2.2 Technologies – Storage

Hydrogen storage technologies are the missing key that scientists and engineers in the early 2000's did not have access to. Hydrogen storage in the form of high-pressure trailer-tubes or cryogenic liquid containers has been known to cause leakage, corrosion, and safety issues. Nevertheless, to understand where each form of hydrogen is best utilised, HBAT models business cases that include the following storage methods: compressed gas, cryogenic liquid, and the more novel approaches—conversion to hydrogen carriers. The LOHC's modelled in this analysis are formic acid, methanol, and methyl formate, along with the inorganic hydrogen carrier ammonia. The production

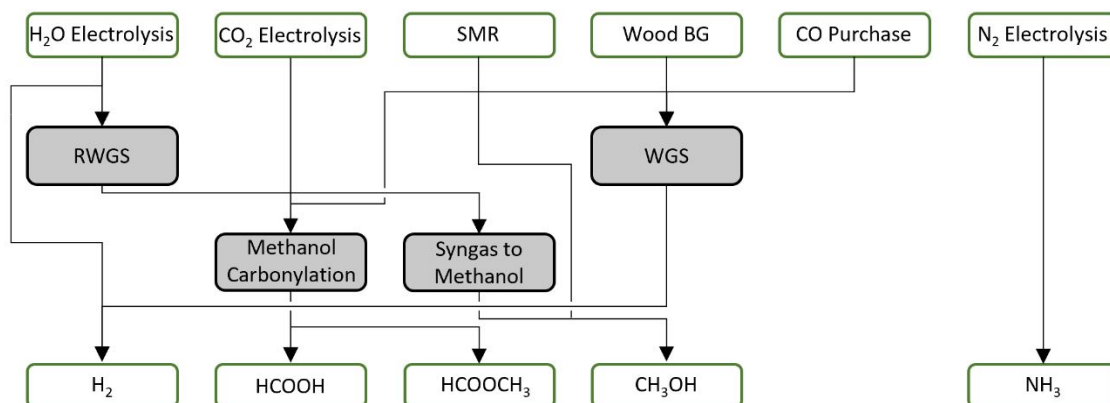


**Fig. 4** Block diagram displaying the path for each supply chain combination between production and storage technologies that HBAT can model. Examples of detailed process flow diagrams for several supply chains are shown in Figure S9 and S10.

technologies that produce CO are directly compatible with LOHC production. Rather than perform WGS, these pathways would simply use the CO product to manufacture the LOHC. The production pathways that do not produce CO, such as water electrolysis, must undergo reverse water-gas shift (RWGS) to first create CO from H<sub>2</sub> and CO<sub>2</sub>. The RWGS economics data was gathered from the Rezaei and Dzuryk techno-economic analysis.<sup>33</sup> All compatible production-storage pathways are exemplified in Figure 4.

Carbon dioxide is a feedstock for electrolysis pathways that create LOHC's. HBAT considers the cost of buying CO<sub>2</sub> as zero, assuming either industry within the vicinity would supply their CO<sub>2</sub> emissions at no cost or CO<sub>2</sub> could be purchased using carbon credits or government subsidies, such as the U.S. 45Q tax credit.<sup>34</sup>

### H<sub>2</sub>

As mentioned previously, hydrogen in the gas or liquid phase is difficult to handle due to its corrosive nature, safety, and density. If one wanted to send gaseous hydrogen in bulk to a different facility without a direct pipeline, the only acceptable options are tube-trailer trucks and tube-rail cars. Due to the excess weight carried by the tube material, a single truck and railcar can only transport around 180 kg and 450 kg of compressed hydrogen respectively. This would incur excessive shipping costs and fuel emissions that other commodities do not have to concern themselves with. An alternative option is to liquefy the hydrogen at cryogenic temperatures to increase the carrying capacity of the truck or railcar. This solves one problem but creates another—hydrogen liquefaction consumes up to 11 kWh kg<sup>-1</sup> of electricity<sup>35</sup> and increases the levelised investment cost by approximately 0.60 USD kg<sup>-1</sup>. Thus, the best use-case for gaseous hydrogen is transported by pipeline; however, shorter, high-capacity pipelines are most economical. Long distance pipelines incur costs nearly proportionally with length, which in some cases may be too great to rationalise.

Due to the issues discussed, certain transportation pathways are not suitable for gaseous or liquid hydrogen. Gaseous hydrogen tube-trailer trucks incur a levelised cost of nearly

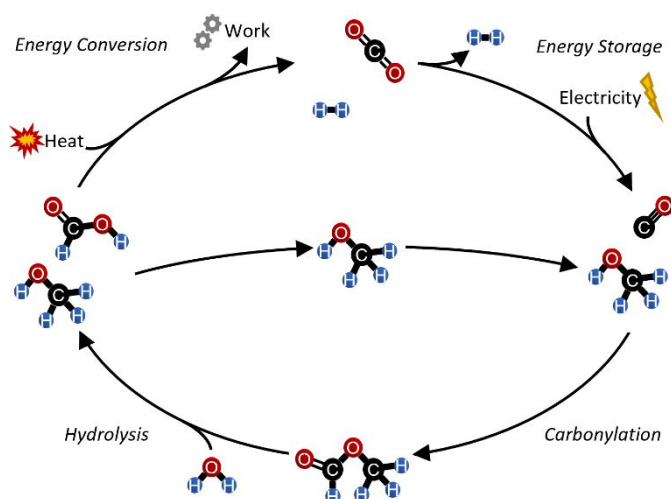
double that of the tube-railcar, and pipelines are costly even without considering cryogenic conditions. For these reasons, our analysis restricts gaseous hydrogen to be transported by pipeline and railcar, while liquid hydrogen is transported by truck and railcar.

Hydrogen derived from PEM water electrolysis is very pure—greater than 99.99%—and as such does not need further purification.<sup>22</sup> All other sources of hydrogen require a purification step that entails sweet/sour amine separations, pressure-swing adsorption, or both. At utility scale, these processes do not make up a significant portion of the levelised cost of hydrogen, nevertheless, the built-in purity is an important property to consider particularly at smaller scales.

### Formic Acid

Arguably the most versatile LOHC, formic acid is known for its ability to be decomposed on demand to hydrogen and carbon dioxide with high selectivity. It has a good volumetric hydrogen storage capacity at 53.5 g H<sub>2</sub> L<sup>-1</sup>, comparable to about 650 bar of pressurised hydrogen. During the 2022 Annual Merit Review, the U.S. Department of Energy Hydrogen Program awarded the University of Southern California and Los Alamos National Laboratory the Storage and Infrastructure Award for their contributions in continuous formic acid dehydrogenation at pressure.<sup>36</sup> The thermodynamics of formic acid dehydrogenation are unique because the reaction is exergonic and mildly endothermic. This allows the reaction to progress, given enough heat, to pressures well above the dew point of carbon dioxide, facilitating purification and compression. The pressure built can then perform work, such as run turbines or pump product through pipelines. Additionally, the state-of-the-art catalyst family<sup>37</sup> used has been proven to maintain its high activity at mild temperatures (90 - 100 °C) over 2.3 million turnovers.<sup>38</sup> Due to these thermodynamic properties, low-temperature waste heat can even be harnessed by this reaction.

While there is no industrial representation of this yet, for the reasons listed above this technology is considered mature enough to warrant significant investment into developing renewable methods to manufacture formic acid. Formic acid is



**Scheme 1** The renewable formic acid hydrogen storage and release cycle. *Energy Conversion*: chemical energy in formic acid and heat is combined to simultaneously create hydrogen and perform work; *Energy Storage*: carbon dioxide is electrochemically reduced using renewable electricity to carbon monoxide; *Carbonylation*: recycled methanol is carbonylated by renewable carbon monoxide; *Hydrolysis*: methyl formate is decomposed with water to regenerate the methanol and produce formic acid.

produced industrially by the carbonylation of methanol and subsequent hydrolysis of the methyl formate ester. While there are several research groups studying the direct electrolysis of carbon dioxide to formate salts, the simpler path would be to use existing manufacturing experience and provide renewable carbon monoxide and energy. Coincidentally, most hydrogen-producing processes already involve carbon monoxide in the form of syngas. When syngas is generated, typically the manufacturer will include a WGS reactor to convert the rest of the CO to CO<sub>2</sub>, generating more hydrogen in the process. To produce formic acid these processes would simply divert the syngas to a RWGS reactor to use the CO to carbonylate methanol. For renewable formic acid production, the CO or syngas could be sourced from CO<sub>2</sub> electrolysis, microbial photoelectrolysis<sup>39</sup> or reforming,<sup>40</sup> or a biodiesel gasification process.<sup>41</sup> In this analysis, we found that CO<sub>2</sub> electrolysis is the most mature technology, and as such this is the only truly renewable direct source of carbon monoxide HBAT considers.

#### Methyl Formate

Methyl formate is an LOHC that is underexplored relative to its acid counterpart yet is full of thermodynamic potential. Methyl formate's volumetric hydrogen capacity alone is appealing at 65.9 g H<sub>2</sub> L<sup>-1</sup>, but the potential lies in the dehydrogenation pathway (Scheme 2). Methyl formate is dehydrogenated by first hydrolysing the ester to its acid and alcohol components. The Gibb's free energy of formic acid dehydrogenation then carries the dehydrogenation of the alcohol to completion using one water molecule. Counting both water molecules that do not have to be transported along with the methyl formate, one molecule of methyl formate can release four molecules of hydrogen, generating an elite effective-volumetric hydrogen capacity of 131.9 g H<sub>2</sub> L<sup>-1</sup>. While these numbers are still unproven, the potential for methyl formate is strong enough to warrant discussion into the economics of this LOHC. Since a significant portion of the investment cost can be saved by

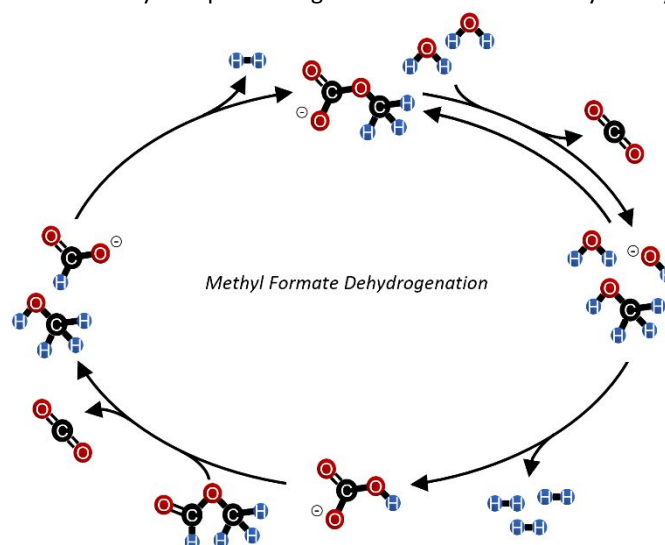
purchasing methanol rather than manufacturing it from syngas, all pathways that use methyl formate only produce CO for the carbonylation reaction. Since the purchased methanol is likely made by SMR, the carbon emissions associated with the methanol are added to the final carbon footprint. The default methanol purchase price is 330 USD tonne<sup>-1</sup>.

#### Methanol

When the hydrogen economy was losing traction, the methanol economy found its place as an analogous concept, using methanol fuel cells and methanol combustion engines to support the energy infrastructure. Due to substantial R&D investment into methanol synthesis and dehydrogenation, there is plenty of experimental data describing how methanol could be used as an LOHC.<sup>42</sup> Unfortunately, the conclusion most have come to is that methanol must be assisted by an alkaline catalyst or stoichiometric reagent in order to dehydrogenate to completion.<sup>43</sup> These alkaline conditions prevent evolution of carbon dioxide, accumulating carbonates that inhibit the reaction. The high volumetric hydrogen capacity of 99.9 g H<sub>2</sub> L<sup>-1</sup> has continued to intrigue investigation, but the reality is that liquid-phase methanol dehydrogenation does not have the goldilocks thermodynamic properties that other LOHC's have. Nevertheless, additive-free methanol dehydrogenation is included in this business case analysis because there are still many that believe the methanol puzzle can be solved.

#### Ammonia

While ammonia is not the most versatile hydrogen carrier, it is the most mature hydrogen storage technology. This is due to the decades of ammonia synthesis research dating back to 1909 when the HB process was conceptualised.<sup>44</sup> Ammonia has an unbeatable volumetric hydrogen capacity at 119.9 g H<sub>2</sub> L<sup>-1</sup> at its boiling point and the dehydrogenation technology is effective and mature. While the thermodynamics are not as favourable as that of formic acid, there are conditions above 350 °C that push the equilibrium to >98% conversion.<sup>26</sup> The only industrially relevant way to produce green ammonia currently is by



**Scheme 2** The methyl formate dehydrogenation pathway. Includes the coupled formic acid and methanol dehydrogenation reactions.

coupling renewably sourced water electrolysis to the standard HB process, however, electrochemical N<sub>2</sub> reduction R&D is advancing rapidly and could be the future of green ammonia production. The 2019 study by Gomez and co-workers compares the economics and sustainability of both; they found that electrochemical N<sub>2</sub> reduction in the presence of hydrogen provided the lowest levelised cost of ammonia. For this reason, this pathway was chosen as the best-case scenario for green ammonia production, with the assumption that future R&D will mature the process.

### 2.3 Technologies – Transportation

HBAT has economic and environmental information for four different fluid transportation methods: pipeline, trailer truck, rail car, and shipping barge. For the scope of this analysis, two transportation methods were used per supply chain depending on whether a pipeline or truck is more appropriate for the hydrogen storage medium. When electricity is required for transport such as with pumps or compressors, the electricity is assumed to be purchased at 0.07 USD kWh<sup>-1</sup>.

#### Pipeline

All hydrogen storage mediums are compatible with the pipeline transportation method except for liquid hydrogen. Liquid hydrogen must maintain temperatures below -200 °C; insulating and cooling even just dozens of kilometres of pipeline would be excessively expensive and energy-draining. Therefore, HBAT makes the conservative assumption that each medium demands the same requirements as gaseous hydrogen in a 316L stainless steel pipeline. Gaseous hydrogen is much less dense and viscous than any of the hydrogen carriers, therefore the pipeline will be priced at a larger diameter than with liquid mediums. This ensures that unforeseen costs such as unexpected corrosion, leaks, and plugs will be covered by the extra cost of pricing out a larger pipeline.

Every pipeline modelled in HBAT is priced by the Argonne National Laboratory HDSAM algorithm,<sup>45</sup> as shown in Equations 1 – 4. The hydrogen pipeline has a defined inlet and outlet pressure. To provide convenient compressor feeds, an outlet pressure of 700 psi was chosen. After brief trial and error, the inlet pressure of 1,000 psi was chosen to optimise the pipeline diameter. The pumps or compressors used to move the hydrogen medium through the pipeline are priced out by calculating the power requirement (Eq. S1-S3). The compressors, used with gaseous hydrogen, are designed using

$$(1) \quad \ln D = A_1 \left[ A_2 \ln (A_3 \dot{M}) + \ln \left( \frac{9T \rho_{rel}^{A_4} \cdot L \cdot Z_{LM}}{5(P_{in}^2 - P_{out}^2)} \right) + A_5 \right]$$

$$(2) \quad Z_{LM} = \frac{Z_{in} - Z_{out}}{\ln \left( \frac{Z_{in}}{Z_{out}} \right)}$$

$$(3) \quad Z_{in, out} = \sum_{n=1}^{n=4} [(B_{2n-1} \cdot P_{in, out} + B_{2n}) \cdot T^{4-n}]$$

(4)

$$IC_{pipeline} = 1.1 \cdot (C_1 \cdot e^{C_2 D} + C_3 D^2 + C_4 D + C_5)$$

#### Definitions

$D$	Pipeline inner diameter (in or m)
$\dot{M}$	H <sub>2</sub> mass flow rate (kg day <sup>-1</sup> )
$T$	Fluid temperature (K)
$\rho_{rel}$	Relative density at 1 atm $\left( \frac{\rho_{H_2}}{\rho_{air}} \right)$
$L$	Pipeline length (mi or m)
$Z_{in, out}$	H <sub>2</sub> compressibility factor at inlet/outlet
$P_{in, out}$	Pressure at inlet/outlet (psi)
$IC_{pipeline}$	Installed cost of pipeline (USD mi <sup>-1</sup> )
$\rho$	Fluid density at 1 atm, 25 °C (kg m <sup>-3</sup> )
$V$	Fluid velocity through pipeline (m s <sup>-1</sup> )
$f$	Turbulent friction factor
$\epsilon$	Pipeline roughness (m)
$Re$	Fluid Reynold's Number
$A_i, B_i, C_i$	Fluid property and pipeline cost constants

(Table S1)

two stages and one spare. The pumps, used for the liquid hydrogen carriers, are sized with one stage and one spare. While realistically a large pipeline would have many smaller booster pumps to maintain lower pressures, to keep cost calculations simple HBAT assumes one will elevate the head pressure enough to pump the fluid through the entire pipeline. The pressure drop calculation is shown in Equations 5 and 6.

$$(6) \quad \Delta P = \frac{f \rho V^2 L}{2D}, \text{ where } f \text{ is estimated by}$$

$$\frac{1}{\sqrt{f}} = -2 \log \left[ \frac{\epsilon}{3.7 D} - \frac{5.02}{Re} \log \left( \frac{\epsilon}{3.7 D} + \frac{13}{Re} \right) \right]$$

*Truck*

Shipping by truck is a common and versatile method of transporting material when other more efficient methods do not exist, or destinations frequently change. This transportation method has two major costs associated with it: the investment cost and the operating cost. HBAT calculates how many trucks need to be in operation at any one moment, determined by the truck carrying capacity and production rate. The truck carrying capacity for liquids is assumed to be 80,000 lb or 8,000 gal, whichever limit is reached first. Each type of truck is priced out by parts: the undercarriage, cab, and intermodal unit. Truck prices vary between 334,000 USD for simple flammable liquids to 915,000 USD for cryogenic liquid hydrogen (Table S2). The lifetime of all trucks is assumed to be 6 years driving 24 hours per day, 350 days per year, with 2-hour loading stops at each destination. The operating costs for the trucks are governed mostly by driver wage, fuel consumption, average speed, and idling time (Eq. S4).

#### Railcar

Shipping by rail is one of the most economical methods of transporting material in the United States. A 2016 report published by the U.S. Department of Transportation<sup>46</sup> clearly described the cost of purchasing new flammable-liquid railcars and their carrying capacities. The 140,000 USD tank cars were used as the base cost, with compressed hydrogen tube cars and

cryogenic liquid hydrogen tank cars costing 549,000 USD and 915,000 USD respectively. The operating costs for railcars vary depending on location and demand, but the average freight cost is 0.04 USD per tonne per mile. HBAT calculates how many railcars need to be purchased, similarly to that of the truck calculation, and what the monthly freight charge accrues to.

## 2.4 Technologies – End-use

Within HBAT, the end-use selection determines the product hydrogen quality requirement, supply-to-demand distance, and predicted demand for hydrogen over the course of the business timeframe. In this analysis, the manufacturing location was selected to be Chambers County, TX, USA. To reduce the number of combinations, only two end-uses were selected: Fuel-cell electric vehicle (FCEV) filling and fertiliser manufacturing. These demand functions vary quite drastically, as shown in Figure 5. NREL expects ammonia production to grow by 15% by 2050. Despite this modest growth, HBAT takes a conservative estimate for hydrogen demand growth for two reasons: 1) fertiliser manufacturing businesses would need to purchase renewable hydrogen at a relatively high price of 7.00 USD kg<sup>-1</sup> and 2) there is uncertainty in whether government subsidies, if provided, would cover the cost of purchasing renewable hydrogen to meet growing fertiliser demand. Although we do not foresee stagnant hydrogen demand by any means, given the reasons stated, we do not anticipate a proportional growth of external hydrogen purchases for fertiliser manufacturing. Thus, HBAT takes a very conservative estimate of a 1.1% total increase in demand for hydrogen by the year 2050. In contrast, FCEV demand has an exponential growth rate because as more hydrogen becomes available, more consumers will invest in FCEVs, creating a positive feedback loop that grows the demand exponentially until the market is saturated. For this reason, the U.S. DOE has predicted that under a high electrification assumption, hydrogen FCEVs will compose 41% of all vehicles by 2050. Using EV LDV future mileage predictions per county from NREL, HBAT calculates the number of miles predicted to be driven by FCEVs through 2050.

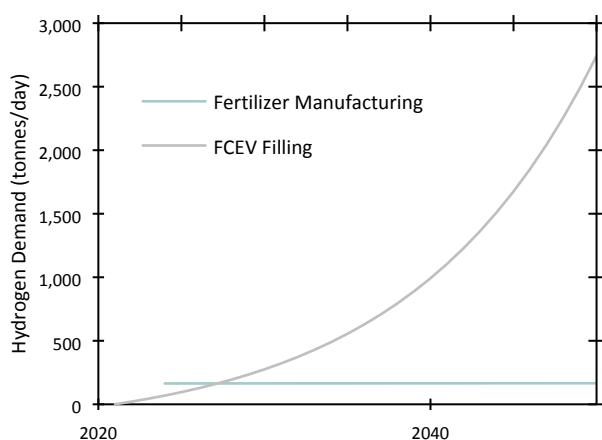
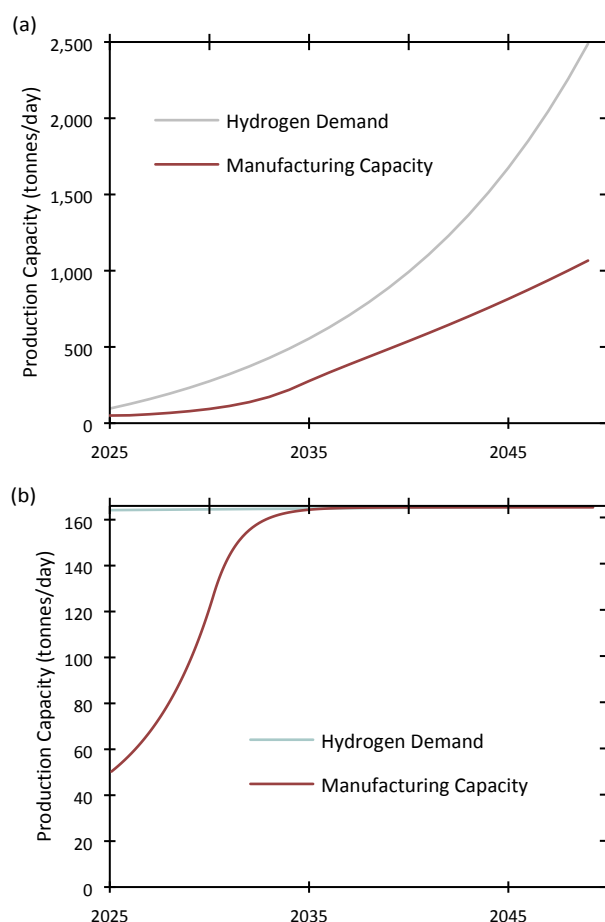


**Fig 5** Hydrogen demand functions over time for a manufacturing plant in Chambers County, TX as predicted by the Energy Information Administration.



Assuming an FCEV efficiency of 51 miles kg<sup>-1</sup>, the county's FCEV

**Fig. 6** Manufacturing capacity growth functions for a biomass gasification scenario. (a) FCEV filling end-use, 511.8-mile transportation distance; (b) Fertiliser manufacturing end-use, 49-mile transportation distance.

demand for hydrogen can be determined. The economic model is discussed in detail in Section 2.6, but in brief, HBAT uses the demand functions to determine how much of the available market the business can expand into. Figure 6 shows examples of two biomass gasification scenarios, the only change being the end-use. Due to the existing fertiliser demand for hydrogen, scenario 6(b) can initially grow quicker but plateaus rapidly. 6(a) has slow initial growth, however, in 2033 the manufacturing capacity surpasses that of 6(b) and continues to grow greater than five-fold. Additionally, due to the specific locations and product quality that FCEV hydrogen requires, there are larger investment and operational costs that do not exist for the fertiliser scenario i.e., extra railcars, a 700-bar compressor, and a CO scrubber.

## 2.5 Scenarios

Of the 1092 distinct supply chain combinations that HBAT can model, we selected 64 that we consider most relevant and applicable. Figure 7 shows these supply chains in a colour-coded visual format and the full list can be found in Table S3. These 64 **supply chains** are modelled using default financial parameters, then six different parameters are modified one at a time for a

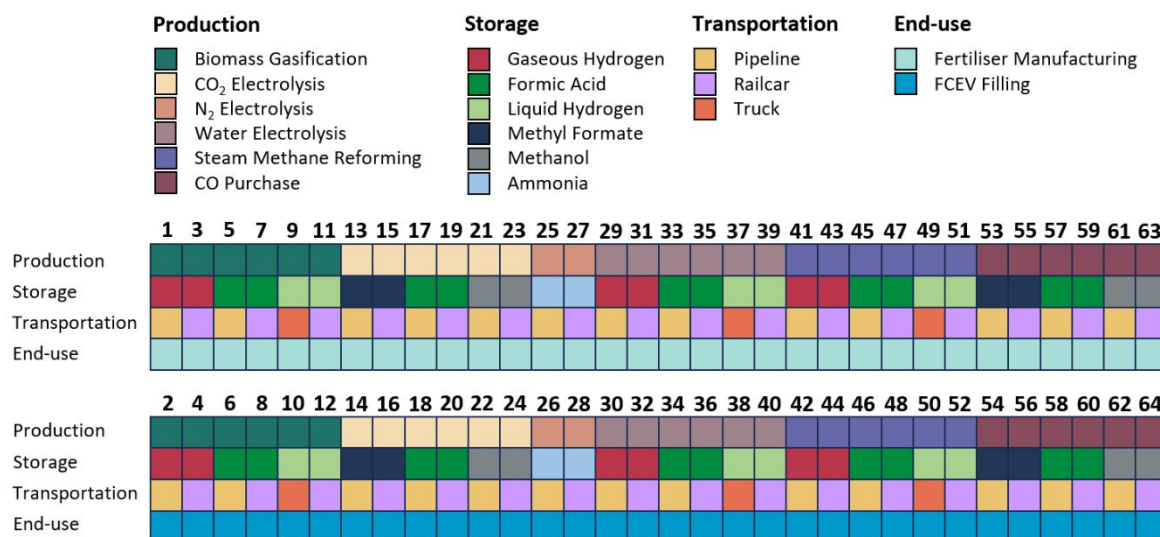


**Fig. 7** Visualisation of all 64 supply chain combinations as 4-block columns. Top layer are production pathways, second layer are storage pathways, third layer are transportation pathways, and bottom layer are end-use cases. The numbers on each column can be used to reference the technologies to their supply chain. Refer to Table S2 for the detailed list.

total of 824 *scenarios*. All scenarios with the specified following parameters were modified: electrolyser longevity, feedstock cost, initial production scale, reinvestment rate, discount rate, parameters and supply chains are listed in Table S4. The and cost of water. These parameters were chosen to convey to researchers and investors how the economic case for hydrogen could change over the next 25 years if various technological, economical, or societal decisions are made. For combinations where a certain parameter is irrelevant, that parameter is ignored – for example, electrolyser longevity is not relevant for biomass gasification. Feedstock cost is a parameter that changes the price of the major energy source. The energy source can be electricity, fuel, or a chemical. In a biomass gasification scenario, the energy source would be the gasified pine wood; thus, the feedstock price would be the price of the pine wood. Similarly, in a CO<sub>2</sub> electrolysis scenario, the energy source is electricity, and the feedstock price would be the electricity price paid to do the electrolysis. The initial production

scale is the production rate that the proposed plant is sized for. Given the reinvestment rate is non-zero, all scenarios use reinvested earnings to increase the production scale of the plant; this scaling is limited by the amount of earnings and hydrogen demand for that end-use at that point in time. This scaling function is also where the reinvestment rate parameter affects the economics. The reinvestment rate is the maximum scaling percentage of the difference between hydrogen demand and production rate. For example, the hydrogen demand is 50,000 kg day<sup>-1</sup> while production is 30,000 kg day<sup>-1</sup>, so a rate of 20% limits the amount of scaling to a maximum monthly increase of 4,000 kg day<sup>-1</sup> given there is sufficient earnings. The discount rate is not a complete scenario change as it does not affect all economic parameters. The discount rate is used simply to calculate the 25-year net present value (NPV). Lastly, the cost of water is varied to simulate how different water supply effects could disturb the hydrogen economy. The technical definitions and relationships between each one of

**Table 2** All parameter combinations modelled in HBAT assigned to their respective scenario range. Refer to supplementary data spreadsheet for complete results table.

Scenarios	< 64	< 92	< 120	< 184	< 248	< 312	< 376	< 440	< 504	< 568	< 696	< 760	< 824
Production Methods													
Electrolyser Longevity	10	20	40	10	10	10	10	10	10	10	10	10	10
Feedstock Price	Low	Low	Low	Med	High	Low							
Production Scale	50	50	50	50	50	25	100	50	50	50	50	50	50
Reinvestment Rate	20%	20%	20%	20%	20%	20%	20%	0%	40%	20%	20%	20%	20%
Discount Rate	8%	8%	8%	8%	8%	8%	8%	8%	8%	6%	12%	8%	8%
C <sub>water</sub> USD t <sup>-1</sup>	1.60	1.60	1.60	1.60	1.60	1.60	1.60	1.60	1.60	1.60	1.60	5.00	10.00

these economic parameters are described in the following section. All variable parameters and their combinations are shown in Table 2.

## 2.6 Economic model

HBAT's economic model is fundamentally a simulation of how the business' earnings will be used and what consequences those decisions create. Seventy unit-operations and equipment items are coded into HBAT, each with distinct cost-scaling functions. When users input their preferred parameters, HBAT calls on each equipment item necessary to link the four supply chains together and scales the costs appropriate to the user's initial production scale. Using an integrated CAPEX estimate tool, HBAT then calculates initial and operating costs by making several industry-standard assumptions. These assumptions are quantitatively described in Equations 7 through 21.

$$(7) \quad C_{mat} = x_{mat} \cdot C_{equip}$$

$$(8) \quad C_{direct} = C_{equip} + C_{mat}$$

$$(9) \quad C_{installed} = C_{direct} + C_{labor}$$

$$(10) \quad C_{Engineering} = 0.09 \cdot C_{installed}$$

$$(11) \quad C_{cont.} = 0.1 \cdot (C_{installed} + C_{Eng'g}) + x_{pro.} \cdot C_{installed}$$

$$(12) \quad C_{BM} = C_{installed} + C_{Eng'g} + C_{conting}$$

$$(13) \quad C_{TP} = \sum_i C_{BM,i}$$

$$(14) \quad C_{TO} = C_{TP} + C_{Owner's}$$

$$(15) \quad OPEX_{Prop. Taxes \& Insur.} = 0.02 \cdot C_{TP}$$

$$(16) \quad OPEX_{Op. Labor} = 3.36 \cdot W \cdot N_{work} - hrs \text{ per year}$$

$$(17) \quad OPEX_{Maint. Mat. \& Labor} = 0.028 \cdot C_{TP}$$

$$(18) \quad OPEX_{Maint. Labor} = 0.35 \cdot OPEX_{Maint. Mat. \& Labor}$$

$$(19) \quad OPEX_{Over head L.} = 0.25 \cdot (OPEX_{M.M.\&L.} + OPEX_{M.L.})$$

$$(20) \quad OPEX_{lab.} = OPEX_{Op. L.} + OPEX_{M.M.\&L.} + OPEX_{Ov. L.}$$

$$(21) \quad OPEX_{fixed} = OPEX_{P.T.\&L.} + OPEX_{labor}$$

Once the day zero Variable OPEX, Fixed OPEX, and Total Overnight Cost ( $C_{TO}$ ) are calculated, the cash flow analysis tool propagates the earnings each month using the user-defined revenue streams. Inflation is not considered so all dollar amounts are reported as 2022 USD. As mentioned previously, the monthly hydrogen demand is used to determine how much production can be increased by reinvesting the monthly earnings. Equations 23 – 25 and 27 show this calculation –  $\%R_1$  is the maximum proportion of EBITDA that can be invested. The default is set to 100%, but a higher percentage could be used. The average plant lifetime is used to calculate the monthly depreciation cost, which is subtracted from net earnings. This affects the payback period, though it is not included in the Cash Flow Present Value (CFPV). Depreciation is instead summed up and subtracted directly from the Equipment & Material (E&M) cost to calculate the plant's residual value. The Plant Residual Present Value (PRPV) is calculated by discounting the opportunity cost from the plant residual value. The 25-year NPV is then calculated by adding the CFPV sum and the PRPV and subtracting the  $C_{TO}$ . A negative NPV can be explained by one of

### Definitions

$x_{mat}$	Proportion of equipment cost for material
$x_{pro}$	Process contingency rate (10-20%)
$C_{Owner's}$	Cost associated with initial inventory
$W$	Operator labour wage (USD hr <sup>-1</sup> )
$D_N$	Hydrogen demand at month N
$P_N$	Hydrogen production at month N
$L_i$	Equipment item lifetime
$CF$	Capacity factor
$C_{TI}$	Total installed cost
$C_{C\&RE}$	Construction and real-estate cost
$\%RR$	Reinvestment rate
$\%R_i$	Financial rate parameters (Table S1)
$C_{I,N}$	Investment cost at month N
$C_{D,N}$	Depreciation cost at month N
$C_{tax,N}$	Income tax at month N (29.2%)
$\%D_N$	Cumulative discount rate at month N
$C_{BE}$	Hydrogen break-even price
$C_L$	Levelised cost of hydrogen

$$(22) \quad EBITDA = Revenue - OPEX$$

$$(23) \quad \Delta P_{D,N} = \frac{D_N - P_{N-1}}{D_N} \cdot \%RR$$

$$(24) \quad \Delta P_{E,N} = \frac{\%R_1 \cdot EBITDA_{N-1}}{C_{TI} - C_{C\&RE}} \cdot (1 - \%R_2)^{\frac{N-1}{12}}$$

$$(25) \quad P_N = P_0 \cdot \min(\Delta P_{D,N}, \Delta P_{E,N}) + P_{N-1}$$

$$(26) \quad \bar{L}_{plant} = C_{TP} \cdot \left( \sum_i \frac{C_{BM,i}}{365 \cdot P_0 \cdot L_i \cdot CF} \right)^{-1}$$

$$(27) \quad C_{I,N} = \frac{P_{N+1} - P_N}{P_0} \cdot (C_{TI} - C_{C\&RE}) \cdot (1 - \%R_2)^{\frac{N}{12}}$$

$$(28) \quad C_{D,N} = C_{D,N-1} + \frac{C_{I,N}}{12 \cdot \bar{L}_{plant}}, C_{D,0} = \frac{C_{TI} - C_{labor}}{12 \cdot \bar{L}_{plant}}$$

$$(29) \quad E_N = EBITDA_N - C_{D,N} - C_{tax,N}$$

$$(30) \quad Net \ Cash = \sum_N E_N$$

$$(31) \quad CFPV = \sum_N \frac{EBITDA_N - C_{tax,N}}{\%D_N}$$

$$(32) \quad PRPV = \sum_N \frac{C_{I,N} \cdot (C_{TI} - C_{C\&RE}) - C_{TO} \cdot C_{D,N}}{C_{TO} \cdot \%D_{max}}$$

$$(33) \quad NPV = CFPV + PRPV - C_{TO}$$

$$(34) \quad C_{BE} = \frac{C_{H2} \cdot (OPEX_N + C_{D,N})}{Revenue_N}, N/12 = 25$$

$$(35) \quad C_L = \frac{C_{H2} \cdot (OPEX_N + C_{D,N})}{Revenue_N}, N/12 = 1$$

the following: a) the plant did not produce sufficient cash in the early stages of the business, b) the depreciation cost outweighed the CFPV by creating a negative PRPV, or c) the  $C_{TO}$  is simply too great. These intermediate finance calculations are described in Equations 22 through 35.

The 25-year NPV was chosen rather than 15- or 10-year NPVs because energy plants require large investments that yield dividends over extended periods. Clearly, no energy plant should be constructed with the intention to liquify the plant prior to 25 years. The payback period HBAT calculates is simpler than a typical present-value calculation done for single pieces of equipment. The net cash earned by the business is calculated by subtracting the sum of monthly depreciation and taxes paid from the sum of EBITDA. The  $C_{TO}$  is then subtracted from the sum to calculate the Return on Investment (ROI). Once the ROI becomes positive, the time in years is recorded as the payback period. Discount rates are not used to calculate ROI because the 25-year NPV already describes a time-value calculation using the discount-rate model. The ROI and payback period are presented as more raw forms of profitability that allow the user to consider their own environmental and socioeconomic principles. Similarly, the break-even hydrogen price is not to be misinterpreted as the levelised cost of hydrogen. The break-even price is a price calculated at year-25 that corresponds with the amount of revenue that offsets every operating cost and depreciation. This price serves more as a point of reference than an actual value for any cash flow calculations. Its purpose is to assist in evaluating the long-term profitability of the business. The last economic variable reported by every scenario is the Earnings Before Interest, Taxes, Depreciation, and Amortisation (EBITDA). This variable is used by investors and financial consultants for nearly every business as a measure of crude earnings. By eliminating financing and accounting manipulations that may benefit some well-established businesses and not others, EBITDA is one of the best ways to compare a technology's true value to others.

## 2.7 Environmental model

HBAT's environmental model uses ANL's GREET tool<sup>47</sup> at the core of its calculations to provide a baseline for each technology's emissions. Due to imperfect fits between GREET and the technologies involved in this analysis, many of the emissions models will have varying degrees of accuracy. GREET models transportation technologies quite well, thus the pipeline, truck, and rail car fuel-consumption emissions along with the emissions associated with compression, pumping, and filling are accurate. GREET's database includes a limited number of production technologies that have a direct match, such as SMR, water electrolysis, ammonia dehydrogenation, and methanol production. Formic acid production was modelled as the related acetic acid process while all other emissions data were collected from techno-economic analyses. These emissions calculations are therefore intended to be used as a reference for relative comparisons and are *not* intended to precisely calculate all emissions associated with these business

cases. While GREET provides a plethora of emissions data, the emissions this analysis will focus on are total carbon dioxide emissions, nitroxides ( $NO_x$ ) and sulphoxides ( $SO_x$ ) emissions, and methane/natural gas emissions. HBAT uses the CertifHy certification<sup>48</sup> requirement to assign each qualifying scenario as "Green" or "Low Carbon". The CertifHy certification states that low carbon hydrogen must produce a well-to-gate carbon footprint of less than 36.4 g  $CO_2$  per MJ of hydrogen, assuming the energy content as the LHV. Therefore, each scenario will be labelled as "Low Carbon" if the carbon footprint is less than 4.368 kg  $CO_2$  per kg  $H_2$ , i.e., 76,400 tonnes of  $CO_2$  per year for a daily hydrogen production of 50,000 kg  $day^{-1}$ . Additionally, CertifHy states that if the producer of low carbon hydrogen also uses renewable energy, defined in their Hydrogen Criteria documentation, the low carbon hydrogen produced by the proportionate renewable energy can be labelled as "Green". If the business does not reach the "Low Carbon" threshold, it will be labelled as "Grey" hydrogen. The environmental impact in Section 3.6 contains all scenarios that produce grey, low carbon, and green hydrogen along with the quantity of renewable energy being distributed.

## 3 Results and Discussion

We conducted an in-depth study of various hydrogen scenarios, exploring a wide range of technologies to determine which hydrogen technologies have the greatest potential to grow in the budding hydrogen economy. After a brief screening analysis to distinguish similar technologies, 824 hydrogen business scenarios were selected and modelled, each with various perturbations, as well as an additional 128 boundary scenarios to better understand parameters that showed unexpected effects. Herein, the results provide comprehensive business analytics, including levelised and break-even costs, optimal production capacities, impact of R&D advancements, and considerations for the feedstock and energy supply chain. We recommend referencing Figure 7 for supply chain numbers going forward.

### 3.1 Supply chain screening

There are numerous technologies within the hydrogen production, storage, and infrastructure space. Of the LOHCs we selected, formic acid, methanol, and ammonia have been studied extensively. Methyl formate and dibenzyl toluene, while more specialized, offer unique benefits. Additionally, though ammonia is well studied, there is no clear consensus on which production pathway has the greatest economic potential. This screening analysis aims to elucidate the preferred ammonia production pathway and describes the reason why the chosen LOHC is included in the primary analysis.

Ammonia production has constantly evolved since its conception in 1909. Since the design used in the 1970's, greater than 35% of energy losses have been eliminated.<sup>44</sup> The Haber-Bosch process is energy intensive as it requires conducting reactions at pressures above 150 bar and temperatures above 400 °C. Fortunately, the current state of the art includes efficient heat integration using waste heat from the SMR reactors to maintain HB temperatures and even run compressors. Green ammonia can be produced either by using water

electrolysers in conjunction with the HB process or low-temperature electrochemical reduction of nitrogen. The techno-economic analysis by Gomez and coworkers<sup>25</sup> presented data indicating that the latter had a higher economic ceiling, but scenarios were modelled in HBAT to verify their findings.

To evaluate the economic impact generated by the HB process, HBAT's model was modified to include an ammonia storage method that can be used along with the water electrolysis production method. Using the Smith et al. review<sup>44</sup> on HB process economics, the bare module costs and energy consumption rates were extracted and implemented in HBAT. Figure 8 shows the BEHP and NPV benefits caused by using the electrochemical N<sub>2</sub> reduction rather than HB. The SMR-coupled HB process is energy efficient because of current integration of recovered SMR heat that can then be used with steam turbines to run the large compressors necessary in HB. A similar plan is used for coupling the water electrolysers to the electrochemical reactors that reduce N<sub>2</sub>, shown in the Gomez TEA. However, due to larger capital and operating costs associated with the construction of two distinct plants in series with little heat integration, the electrolysis-coupled HB process presents a significantly weaker business case in every transportation method and end-use modelled. Based on these results, this analysis uses electrochemical N<sub>2</sub> reduction as the optimal production method for ammonia. Though this novel method is chosen, it is important to note that electrochemical N<sub>2</sub> reduction is still primarily an R&D effort and may take much longer to commercialise.

An intriguing LOHC that has gained increasing traction is dibenzyl toluene (DBT). Toluene and some derivatives such as DBT have the reductive ability to store hydrogen along the many aromatic bonds of the molecules. DBT-H<sub>18</sub> has a good hydrogen storage density and volumetric hydrogen density at 6.2 wt% and 63.8 g L<sup>-1</sup>, respectively. However, DBT is expensive and must be maintained in a closed loop system with minimal losses to be feasible. Methyl formate exhibits similar hydrogen storage numbers at 6.7 wt% and 65.8 g L<sup>-1</sup>, but the dehydrogenation results in the production of CO<sub>2</sub>. When electrolysis-sourced methyl formate is dehydrogenated, CO<sub>2</sub> is produced in a

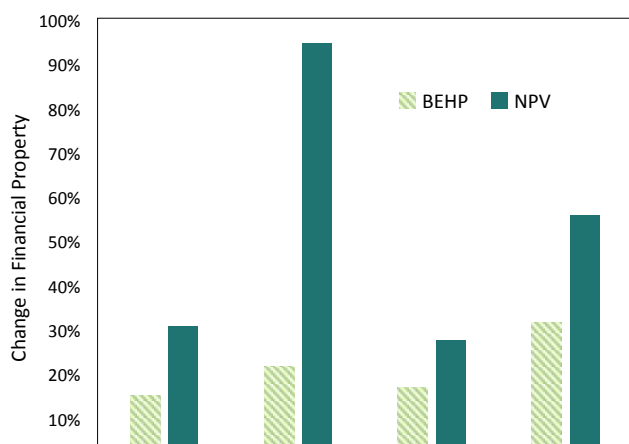


**Fig. 8** Differences between production pathways for hydrogen stored in ammonia. Data show the economic benefits that the electrochemical reduction of nitrogen may provide when compared to the Haber-Bosch process. Striped, green bars show the percent reduction in break-even hydrogen price (BEHP); teal bars show the percent increase in 25-year net present value (NPV).

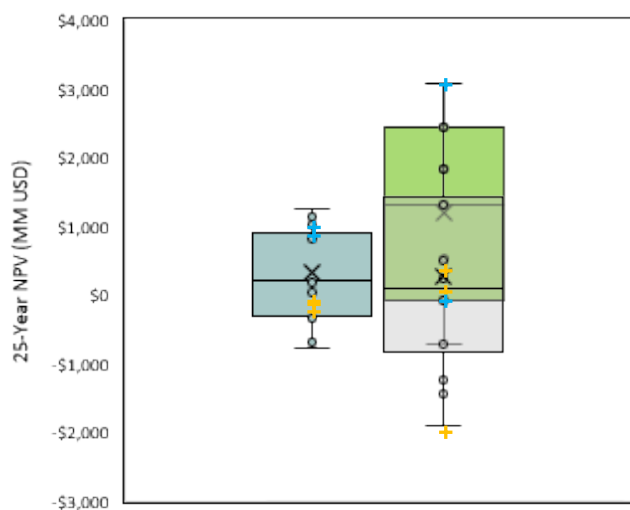


**Fig. 9** Distribution of 25-year net present values for all chemically-stored H<sub>2</sub> supply chains, including six DBT variants. Pale blue box plot (left) represents all fertiliser manufacturing supply chains; grey box plot (right) represents all FCEV filling supply chains; green box plot (right) represents the railcar-FCEV supply chains; yellow points represent DBT supply chains; blue points represent methyl formate supply chains.

carbon-neutral fashion. If a carbon-negative process is desired, the resultant CO<sub>2</sub> may be captured using government incentives. The differences between the LOHCs have dramatic consequences in the infrastructure needed to transport hydrogen; DBT requires round-trip liquid transportation while methyl formate needs only one-way transportation. Because of this, all DBT scenarios modelled in HBAT have much higher CAPEX and OPEX transportation costs.

Six DBT supply chains were modelled: truck, railcar, and pipeline transportation were chosen with fertiliser manufacturing and FCEV-filling end-uses. The Niermann et al. TEA<sup>49</sup> provided economic data for process cost estimates for DBT hydrogen cycling. Despite their conclusion that DBT-H<sub>18</sub> was only able to supply hydrogen at a levelised cost of 13.6 € kg<sup>-1</sup> H<sub>2</sub>, HBAT estimates much lower costs. This is because the authors modelled international transportation by ship over thousands of kilometres, whereas this analysis only considers land transportation up to 824 kilometres.

Figure 9 shows the discrepancy between the NPVs of DBT supply chains compared to other storage mediums. DBT's NPVs are all in the lower half their respective groups. Even the best DBT supply chain, railcar to FCEV-filling, falls short in comparison to the average railcar supply chain. In contrast, methyl formate supply chains are among the best business cases of all carrier supply chains. Even the least efficient methyl formate supply chain performs better than four of six DBT supply chains modelled. While there are less viable supply chains than the six DBT supply chains modelled, closed-loop transport with DBT limits its capability. For this reason, this analysis will only include the LOHCs that can use one-way transportation.

### 3.2 Profitability and levelised cost analysis

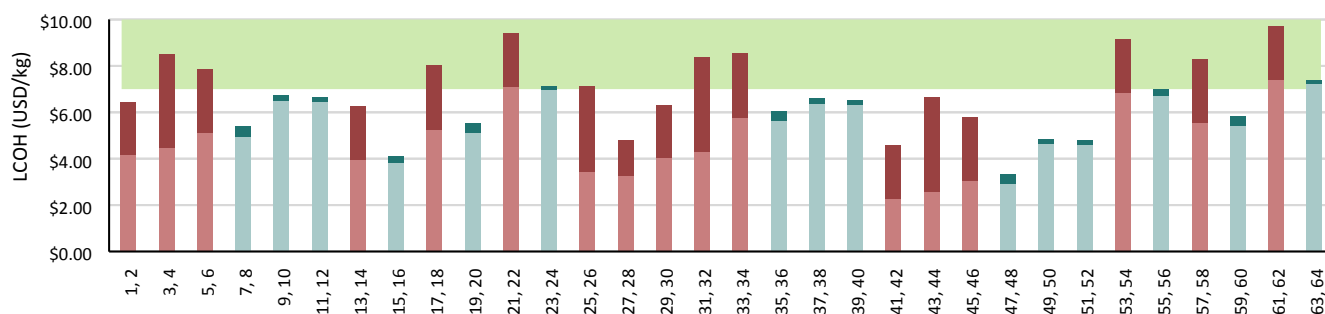


**Fig. 10** Levelised Cost of Hydrogen (LCOH) for all 64 supply chains sized to 50,000 kg/day, grouped into each pair of supply chains varying only end-use. Blue bars represent group 1 supply chains, red bars represent group 2 supply chains. The green box represents the profitability zone at a sales price of 7 USD/kg H<sub>2</sub>. Pale bars represent the LCOH of the fertiliser manufacturing end-use variant while the darker bars represent the extra costs associated with converting to the FCEV filling variant. (Scenarios 377 – 440)

Levelised costs are defined as the costs associated with purchasing and operating a piece of equipment throughout its lifetime partitioned between the number of units of product produced over the same lifetime. In this analysis, levelised costs are defined as the CAPEX and OPEX costs incurred per kilogram of hydrogen produced during the simulated plant's lifetime. One issue with this method is that each piece of equipment has its own distinct depreciation rate, (36) the strategy developed in HBAT combines the lifetimes of every piece of equipment or material into a weighted average. This calculation is shown in Equation 26.

$$PI = \frac{NPV + C_{TO}}{C_{TO}}$$

Observing how the levelised costs vary across the various supply chains, two distinct groups appear. Group 1, named the scalable group, is defined by high initial costs yet low operating costs. Group

2, named the economy group, is defined by low initial costs but high operating costs. Of the 32 pairs of supply chains with varying end-uses, the scalable group consist of the 15 with levelised cost of hydrogen (LCOH) differences that are less than 0.50 USD kg<sup>-1</sup> while the economy group consist of the 17 with differences greater than 1.50 USD kg<sup>-1</sup>. This is visualised in Figure 10 and then shown as a box plot distribution in Figure 11. In general, the scalable group have moderate LCOH's typically (the interquartile range) between 4.58 and 6.74 USD kg<sup>-1</sup>, with little variation in levelised economics between fertiliser and FCEV filling end-use cases. This changes once profit reinvesting is applied. Figure 12 shows the profitability index (PI) distribution of all supply chains when allowed to reinvest at the default rates. The PI, calculated from the ratio between present value and total overnight investment, shows a calibrated result of each supply chain's economic viability. This group's fertiliser cases are somewhat profitable, with PI's typically between 60.3% and

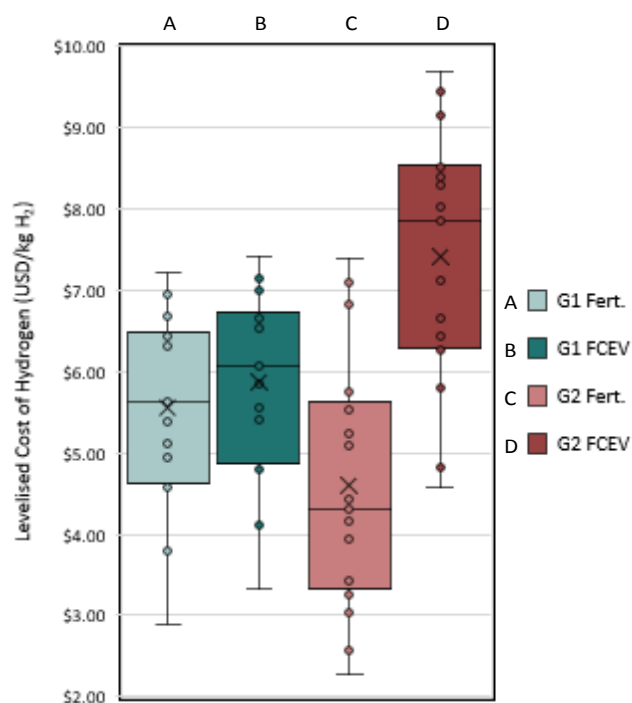


**Fig. 11** Levelised cost of hydrogen distribution among the 64 base supply chains. Grouped into group 1 and 2 fertiliser manufacturing and FCEV filling end-use cases. Bars represent middle (first and third) quartiles, X represents the mean, and the centre line represents the median. The interquartile range is defined as the difference between the first and third quartile.

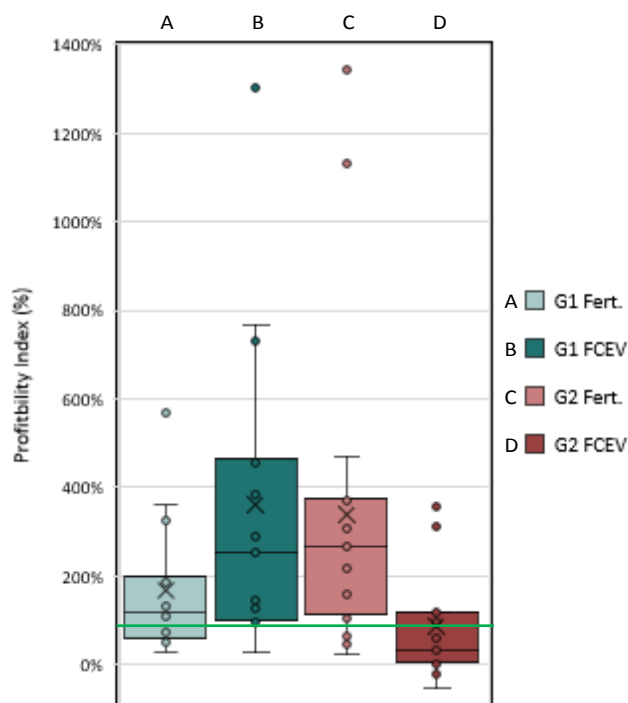


**Fig. 12** Profitability index (PI) of each group and end-use. Green line represents the break-even line, PI = 100%. (Scenarios 1 – 64)

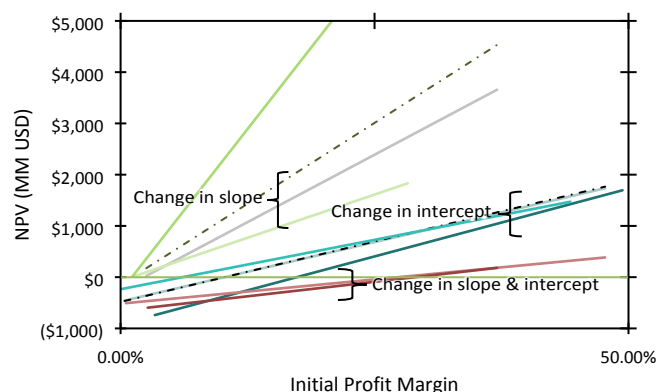


**Fig. 13** NPV achieved for various scaling strategies, plotted against the respective initial profit margin. Only regression lines shown, data can be seen in Figure S1. [end-use, initial daily production, reinvestment rate]: FCEV, 50k, 40% (dashed olive); FCEV, 100k, 20% (green); FCEV, 50k, 20% (grey); FCEV, 25k, 20% (light green); Fert., 25k, 20% (cyan); Fert., 50k, 20% (pale blue); Fert., 50k, 40% (dashed black); Fert., 100k, 20% (dark blue); FCEV, 50k, 0% (dark red); Fert., 50k, 0% (pale red).

193.7%; however, the group's greatest strength is the FCEV cases with PI's typically between 93.4% and 464.9% and the highest mean PI. The economy group have superior fertiliser economics but weak FCEV filling economics. The fertiliser supply chains of the economy group have the highest median PI of all groups but tend to have modest profitability ceilings due to the inability to scale.

Interestingly, the two groups have supply chain patterns that can be recognised. All scalable group storage mediums are either liquid hydrogen or railcar-transported LOHC supply chains. Of the LOHC's found in the scalable group, five are formic acid, two are methyl formate, and two are methanol. Since the scalable group does not contain any gaseous hydrogen, pipelines, or ammonia supply chains, it can be concluded that these technologies are not optimally used for long-distance, high-volume production and transportation of hydrogen such as in the case of FCEV filling. The economy group does have a place in the world's hydrogen economy, but it is most suited for short-distance, low volume production of hydrogen such as in the case for fertiliser manufacturing.

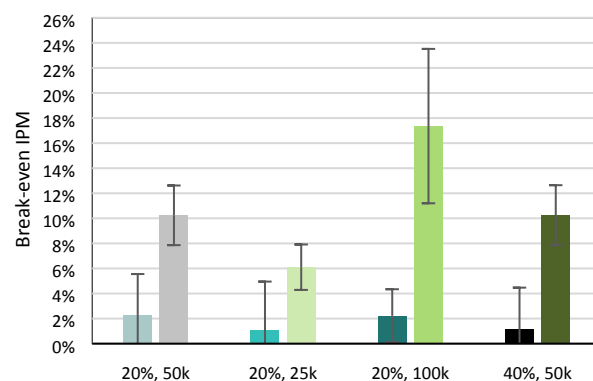
While none of these LCOH's achieved the delivered price of 2.00 USD  $\text{kg}^{-1}$  that is aimed for by the U.S. DOE, the break-even price calculated in Equation 34 shows a more realistic selling price for each supply chain once each business case is matured over 25 years.

### 3.3 Installed capacity analysis

HBAT users can vary the initial capacity the production plant is sized for. Changing this parameter can modify the entire financial model including transport distance, labour, equipment size, and real estate. Furthermore, as described in Section 2.6 and shown visually in Figure 6, the capacity growth depends on factors such as the available hydrogen demand, monthly earnings, total overnight cost, and reinvestment rate (%RR). To explore the model without growth, one set of scenarios (377-440) are modelled using a 0% reinvestment rate. This experiment showed that every supply chain modelled would benefit from reinvesting earnings into increasing production, as shown in Figure 13. The X-intercepts of the regression lines show the break-even initial profit margin (BPM) that must be met for that group of supply chains to achieve a positive NPV. The red 0% investment lines show that there are only minor

**Fig. 14** Break-even initial profit margin. Shown with regression confidence intervals and split into experimental groups. Colours for each group match scheme in Figure 13.

differences between end-uses when reinvestment is not applied. The BPMs of both lines are statistically indistinguishable (85.2% chance of being random error) and the slopes, while likely different, cannot be distinguished using 95% confidence (24.2% chance of being random error). These findings corroborate the qualitative result shown by the similar positions of the two red lines in Figure 13. Interestingly, once reinvestment is introduced, the trends between end-uses diverge; FCEV filling supply chains maintain consistent BPMs between 1-2% while the fertiliser manufacturing supply chains vary anywhere between 6-18%. The NPV slopes of both end-uses tend to increase with increasing initial production, however, the BPMs of the fertiliser supply chains increase dramatically. This negates any potential economic benefit the increased NPV slope may have because of higher risk. Due to this trend, the 25k production capacity variation for fertiliser scenarios could be the most attractive due to the low X-intercept and serviceable NPV slope. The 100k production capacity variation has very little economic benefit. The increase in production exacerbates unproductive scenarios and provides very little benefit to the profitable ones due to the demand ceiling. Meanwhile, the FCEV NPV slopes increase with insignificant change of the BPM (the most significant pair has a 57% chance of being random error). The statistical relationships of each group's BPM and slope are shown in Figure 14 and S2,



respectively. Many FCEV scenarios that would otherwise have a slightly negative NPV are very positive when adjusted to the

**Table 3** Student's paired t-test analysis of payback period and break-even production, comparing the groups for statistical differences. 2-tailed;  $\alpha = 0.05$ ; pass:  $p < \alpha$ ; fail:  $p > \alpha$ . 100k production capacity due to a two- to three-fold increase of initial profit margin. Combined with the additional benefit of achieving greater NPV's per % of profit margin, the 100k production capacity becomes very attractive for FCEV filling supply chains. The variation in optimal initial production capacities for each end-use illuminates the relationship between optimal initial production and market size. It appears that there is an optimal production to market size ratio such that fertiliser manufacturing and FCEV filling at 50,000 kg day<sup>-1</sup> H<sub>2</sub> are on opposite sides of the maximum.

When analysing the payback period (PBP) and break-even production scale (BEP), there is no single factor that can be correlated to each result. Both PBP and BEP depend on multiple variables that cannot be controlled; therefore, we must analyse them by grouping the results and using statistical tests to determine if individual modifications to parameters can cause significant changes on the mean result of the group.

Controlled Parameters	Statistical Test	Result
PBP [25k, 20%]	Fert. (A) vs. FCEV (C) t-test	Pass
PBP [100k, 20%]	Fert. (B) vs. FCEV (D) t-test	Pass
BEP [25k, 20%]	Fert. (E) vs. FCEV (G) t-test	Fail
BEP [100k, 20%]	Fert. (F) vs. FCEV (H) t-test	Fail
PBP [50k, 0%]	Fert. (I) vs. FCEV (K) t-test	Fail
PBP [50k, 40%]	Fert. (J) vs. FCEV (L) t-test	Pass
BEP [50k, 0%]	Fert. (M) vs. FCEV (O) t-test	Pass
BEP [50k, 40%]	Fert. (N) vs. FCEV (P) t-test	Pass

shows the statistical results from comparing each group upon perturbing a single variable, effectively determining whether the modified variable induced a statistically significant change in the group's mean. Passing the test indicates a significant change while failing it can be interpreted as random. The control data represents the same data used to normalise the information in Figure 15. Hence, each control t-test can be compared to the null hypothesis 100% line by analysing the corresponding box plot.

The control vs. **B** plot provides an interesting insight into how the economics of fertiliser scenarios change. **A**'s dataset shows that a decrease in initial production always results in an increase in payback period; however, the opposite is not true when initial production is increased. This is shown visually by the overlapping distributions of both **A** and **B**. This can be explained by the electrolyser scenarios. Electrolysers and solar arrays have minimal per-unit savings when purchasing at larger scales, unlike the vessels, pipelines, and infrastructure that has scaling exponents as low as 0.6. When the plant is sized for double the capacity, many of these scenarios nearly double in C<sub>TO</sub>, and because there isn't much excess demand in fertiliser manufacturing, this capacity expansion does not accelerate the business growth either. Production increase still causes a statistically significant effect in the payback period ( $p = 0.006$ ), but the effect would be clearer without the electrolyser scenarios.

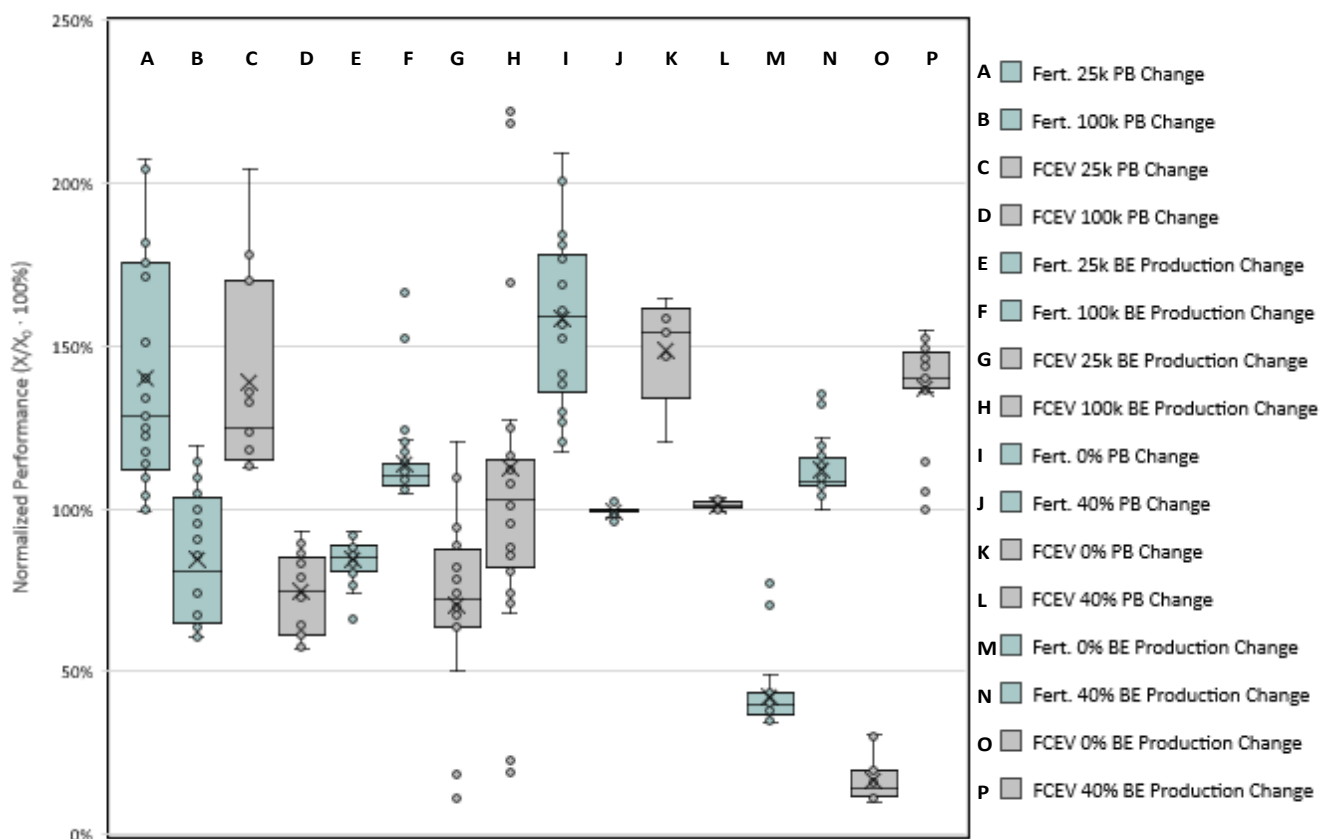
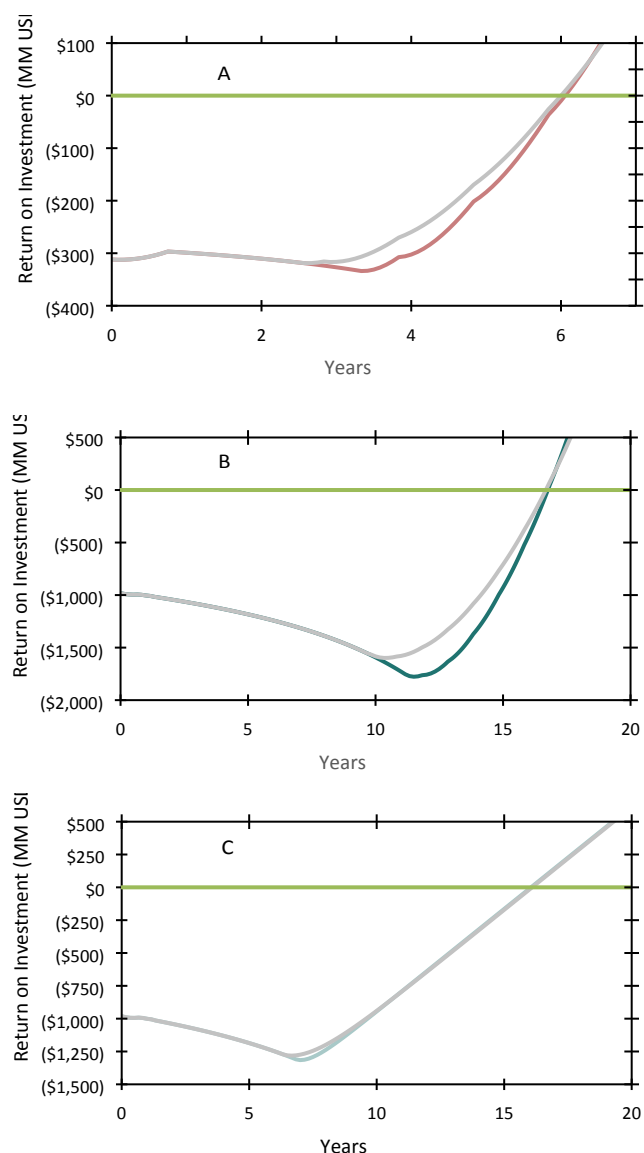


Figure 15 displays the distributions for each set of results, portraying the normalised deltas for each perturbation. Table 3

The FCEV filling counterpart, control vs. **D**, shows a much stronger effect of increasing initial production ( $p = 0.00002$ ).



**Fig. 16** Return on investment plots showing the payback period. The grey scenarios show the default input parameters, using 20% reinvestment and 50,000 kg day<sup>-1</sup> production, and the coloured scenarios compare their 40% reinvestment counterparts. (A) Scenario 48 vs. 488. (B) Scenario 20 vs. 460. (C) Scenario 19 vs. 559.

This is in part due to the growth acceleration enabled by FCEV's growing hydrogen demand, but also the larger proportion of storage and transportation equipment that uses favourable scaling exponents. Despite the overlap shown in the **A** vs. **C** and **B** vs. **D** box plots, the paired t-test shows a statistically significant difference between both pairs of groups. Since this is comparing normalised data, the analysis indicates that the end-use market affects the payback period change caused by perturbing the initial production scale in either direction. The initial investment rate has a greater effect on the FCEV-filling payback period, but both end-uses still have statistically significant benefits. The t-tests for fertiliser control vs. **B** and FCEV control vs. **D** both pass with p-values of 0.006 and 0.00002 respectively.

To reiterate, the reinvestment rate is the proportion of excess demand that is used as a scaling ceiling, regardless of available profit. The 0% reinvestment scenarios were used for the LCOH

analyses earlier, but they are also used to compare how the different end-uses could benefit from reinvestment. The **I** vs. **K** test shows that there is very little difference ( $p = 0.4$ ) in payback period change between end-uses when reinvestment is zero. This indicates that the economics of the business case relies entirely on the production cost at time of investment, such that the business' long-term finances will never benefit from improved technology or growing markets.

The **J** vs. **L** boxplots may seem like they are too similar to distinguish, but in fact the narrow variance enables high statistical significance ( $p = 0.0003$ ). The small variance indicates that while the impact of increasing reinvestment is significant, its impact on payback period is minute. Interestingly, the change in payback period is applied in opposite directions such that payback periods for fertiliser manufacturing decrease with high reinvestment rate, while that of FCEV-filling increase. Figure 16 shows three separate supply chains where the return on investment (ROI) is plotted over time. Figures 16A and 16B both show FCEV-filling supply chains with different CTO's and payback periods. These are representative scenarios that show the effect of increasing the reinvestment rate for FCEV end-uses. Observing only the payback period, one would deduce that 40% reinvestment has little effect on these supply chains; however, these ROI plots show the true effect. Since the reinvestment rate only affects the *maximum* reinvestment, the profit must reach a certain point to diverge from the default scenario. Once this point is reached, the 40% scenario maintains its trend of decreasing ROI until the new max reinvestment occurs, causing the ROI to start increasing. Interestingly, in nearly every case, the two ROI lines for the same supply chain consistently converge soon after the payback period. The benefit of the 40% scenario is the larger rate of return following the payback period. This only occurs for FCEV filling scenarios; as shown by Figure 16C, fertiliser manufacturing scenarios reach a maximum rate of return very quickly after reaching profitability. This prevents the acceleration benefit observed in Figures 16A and 16B.

The break-even production scale can be understood as the minimum production necessary to produce cash profit. It is highly correlated with the production associated with the minima on the ROI plots. Intuitively, the more profitable the scenario at 100% capacity, the sooner this minimum is reached. Figure 15E – H and M – P show the generic trends. Changing the initial production scale of fertiliser manufacturing scenarios causes a correlated effect in the BEP. This pattern is not observed in the FCEV scenarios due to other factors that influence the BEP. The normalised median BEP in FCEV filling scenarios with 100,000 kg day<sup>-1</sup> initial production (plot H) is only at 102%, with the first and third quartiles ranging from 80% to 115%. The 25,000 kg day<sup>-1</sup> variant (plot G) is more distinctive, but the data range still encompasses the null hypothesis. As expected, due to the case-by-case nature of the FCEV filling BEP trend, both the control vs. H test and the F vs. H test fail with p-values of 0.3 and 0.9 respectively.

Reinvestment rate has the most distinct effect on BEP. As more reinvesting occurs such as in Figure 16A and 16B, the time to

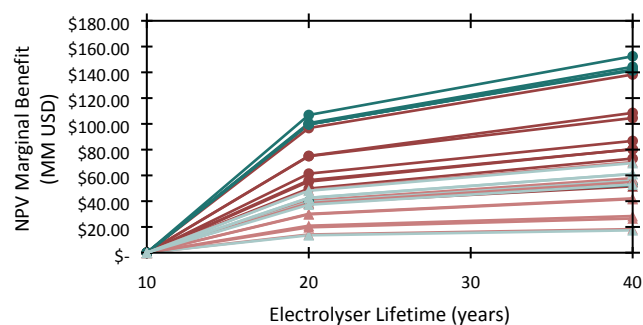


Fig. 17 Net present value functions for each electrolyser supply chain, modifying the electrolyser longevity from default (10 years) to 20 and 40 years: Fertiliser manufacturing (triangles); FCEV filling (circles).

reach the BEP is consistently and predictably delayed. All four BEP-RR tests, **M** vs. **O**, **N** vs. **P**, control vs. **N**, and control vs. **P**, quantitatively corroborate the graphical observations by passing the t-tests with p-values less than  $1 \times 10^{-7}$ .

### 3.4 Electrolyser longevity analysis

Every new business planning to enter a market must consider the lifespan of its technology. This entails maintenance and recalibration labour costs, cleaning material costs, equipment refurbishing costs, material replacement costs, and many other costs that a technology incurs from continuous use. HBAT assumes a general annual maintenance cost as 2.8% of the  $C_{TP}$  (eq. 17), but for each piece of equipment, the supplementary upkeep cost is calculated as an average of the aforementioned costs into a monthly “depreciation” cost (eq. 28). It is calculated using an “average plant lifetime” to determine how many months the plant could theoretically survive without paying the upkeep cost. This cost is not calculated into the OPEX cost, instead it is subtracted from the earnings (EN) and affects the NPV, ROI, and consequently the BEP and PBP.

As described quantitatively by Equation 28, the total depreciation cost is calculated using a weighted average of each individual equipment lifetime. The weight of each lifetime is given by the bare module cost of the particular equipment item. Due to these two factors, the equipment items that affect the depreciation cost the greatest are the items that have the short lifetimes and high bare module costs. Typically, most manufacturing plants avoid technologies that have this property, but electrolysis plants will not be able to avoid it. Electrolysers and fuel cells have notoriously short lifetimes and high costs due to the scarcity of their manufacturing materials and harsh physical and chemical environments. For these reasons, this analysis applies changes to the electrolyser lifetime, simulating how improved technology could impact the business cases of these electrolysis supply chains.

The first and most impactful analysis is determining the effect of extending electrolyser lifetime on the NPV. This will produce a number that can be used to determine how much R&D investment could be implemented to achieve the desired lifetime. Because the scale-up rates, profit margins, and investment costs differ significantly across each scenario,

counter-intuitively, it is not beneficial to compare normalised NPV data. Instead, each scenario should be analysed individually based on NPV differentials, which are shown as functions and distributions in Figure 17 and 18, respectively. The functions in Figure 17 show the diminishing returns from improving the longevity of electrolysers. The supply chain with the greatest benefit of improving electrolyser longevity from 20 to 40 years is only 33 MM USD greater than the supply chain with the least benefit of improving the longevity from 10 to 20 years. In this analysis the boundaries between the scalable and economy groups are not clearly defined, indicating that the R&D benefits can be applicable to any supply chain regardless of end-use, scalability, or total overnight costs. The FCEV filling supply chains typically have the greatest 10-to-20 benefit; however, the methyl formate variants (**14** & **16**) have smaller electrolysers and therefore do not benefit as much as some of the best fertiliser manufacturing supply chains. The pipeline supply chains (**14**, **18**, **22**, **30**, & **34**) also have a diminished benefit due to the small proportion of electrolyser to pipeline cost. All but one FCEV-pipeline supply chains boast total overnight costs greater than 1.3 billion USD. Electrolysers tend to cost between 100 and 300 million USD depending on the supply chain. Interestingly, supply chain **30**, an FCEV-filling and compressed-hydrogen pipeline scenario, achieves a positive 25-year NPV and sees benefits from electrolyser R&D similar to the other railcar and truck supply chains. This is due to its simplicity, since no additional investment needs to be incurred to store the hydrogen, only the compressors and pipeline. Moreover, this supply chain has the lowest break-even  $H_2$  price of any pipeline supply chain at 2.50 USD  $kg^{-1}$  and 2.28 USD  $kg^{-1}$  for a 10- and 20-year electrolyser lifetime, respectively. This indicates that the operating and depreciation costs are low enough to achieve favourable price points after the initial investment.

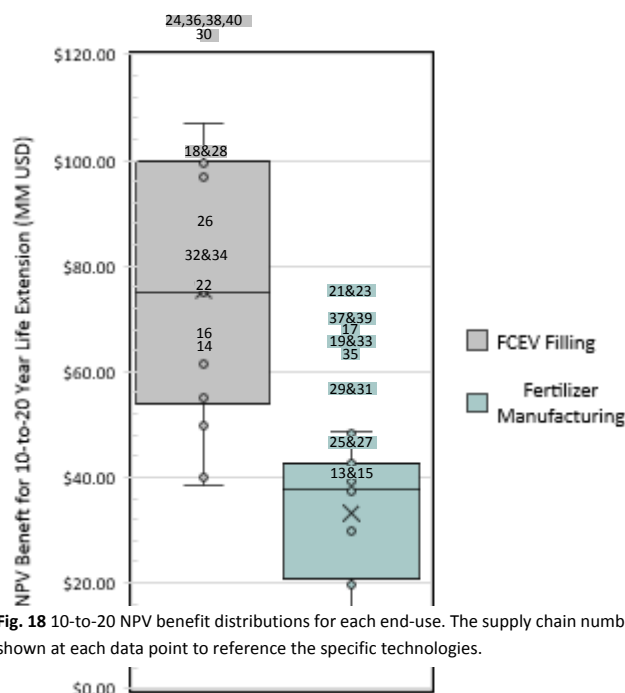


Fig. 18 10-to-20 NPV benefit distributions for each end-use. The supply chain number is shown at each data point to reference the specific technologies.

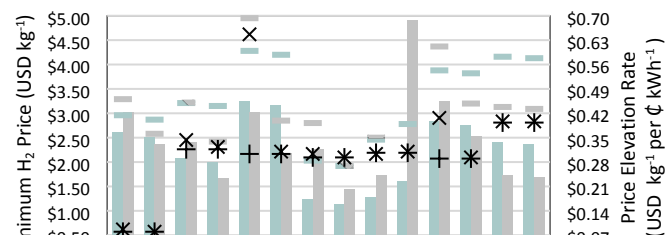


Fig. 19 Linear function parameters for break-even hydrogen price as a function of electricity cost for electrolyser supply chains: the X-intercept, minimum H<sub>2</sub> Price is shown as columns (fertiliser: pale blue, FCEV: grey); the slope, price elevation rate is shown as points (fertiliser: +, FCEV: x). Default break-even H<sub>2</sub> prices shown as appropriately coloured bars, plotted against the left vertical axis.

\* Supply chain 32 break-even H<sub>2</sub> price is off-chart at \$5.80

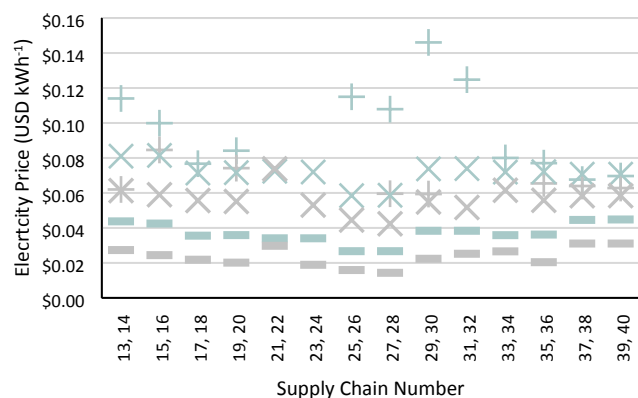
### 3.5 Electrolyser utilisation optimisation

There is a looming problem concerning every investor, government, engineer, and decision-maker when considering electro-chemical manufacturing using renewably sourced electricity. When intermittent power generators supply electricity to the production plant, the electrolyzers must be powered down or even shut down completely during times of low energy generation. In practice, this would prevent full use of all renewable electricity produced because a minimum threshold would be required to maintain normal operation. Additionally, the large proportion of downtime would result in an uncomfortably large opportunity cost. A solution to this problem could be to purchase grid electricity or low-cost dispatch-constrained electricity (LDE) during times of low renewable energy generation. This would stabilise the energy supply-chain and allow the electrolyzers and manufacturing to run at near full capacity even when the generators are running low or shut off. The purpose of this analysis is to discover the opportunity for each supply chain to optimise their electricity sources. Scenarios 133 – 160 and 197 – 224 were used for this study. The electrolyzers are modelled to run for 23 hours a day using 10 hours of renewable electricity and 13 hours of purchased electricity. This effectively reduces the scale of electrolyser required for a given daily hydrogen production thereby reducing CAPEX costs but increasing OPEX costs. Figure S3 shows the %reduction rate for each supply chain's C<sub>TO</sub>, with an average reduction of 32%.

Interestingly, many financial properties of each business case demonstrated perfectly linear relationships with the electricity purchase price, using five electricity prices with supply chain 20 (Figure S4). As a result, the entire function could be determined from two data points. These linear functions include the BEHP, 25-year NPV, IPM, and monthly EBITDA. Figure 19 shows the minimum BEHP ( $C_{\text{electricity}} = 0 \text{ USD kWh}^{-1}$ ) and slope for each electrolyser supply chain as well as the default BEHP to visualise the economic potential of the 23-hour strategy. Notably, there is a significant contrast between the methyl formate supply chains (13-16) and the rest. Because methyl formate supply chains purchase methanol to supply part of the evolved

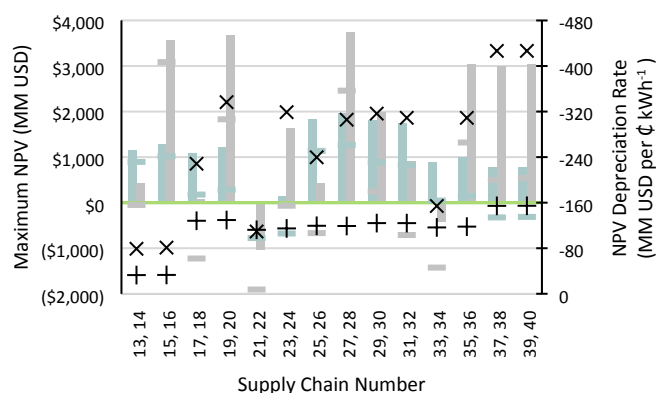
hydrogen, smaller electrolyzers can be used to produce equivalent amounts of hydrogen. This decreases the vulnerability of the business to electrolyser economics, as shown by the nearly four-fold reduction in price elevation rate for both FCEV filling and fertiliser manufacturing end-uses. Another noteworthy observation is the discrepancy in price elevation rates between fertiliser manufacturing and FCEV filling end-uses. Typically, there are very small differences in rates, but for supply chains 21 vs. 22 and 33 vs. 34, the difference is significant. The reasons for this could be attributed to several factors, including the fact that both scenarios involve LOHC-pipelines. The most notable is that supply chain 22 and 34 have the two highest total overnight costs of any electrolyser supply chain. In contrast, the analogous fertiliser supply chains 21 and 33 have dramatically lower total overnight costs, resulting in lower profit margins that affect the BEHP. Figure 19 also reveals that a significant number have minimum BEHPs below 2.00 USD kg<sup>-1</sup>. There are nine total supply chains with the potential to sell clean hydrogen at this competitive price; however, the electricity price margins needed to reach these levels are quite slim, highlighting the need for LDE. The nitrogen reduction supply chains, 25 – 28, exemplify some of the benefits harnessed by this 23-hour strategy. The default fertiliser supply chains 25 and 27 already have some of the lowest BEHPs at 2.03 USD kg<sup>-1</sup> and 1.92 USD kg<sup>-1</sup>, and the reduction in CAPEX diminishes costs enough to lower their minimum BEHPs by 38.4% and 40.6% respectively. These benefits result in a business case where the plant could purchase LDE for up to 0.026 USD kWh<sup>-1</sup> and 0.029 USD kWh<sup>-1</sup> using supply chain 25 and 27 respectively and still sell green hydrogen for less than 2.00 USD kg<sup>-1</sup>.

Fig. 20 Linear function parameters for net present value as a function of electricity price for electrolyser supply chains: the X-intercept, maximum NPV (fertiliser: pale blue, FCEV: grey); the slope, NPV depreciation rate (fertiliser: +, FCEV: x). Default NPV shown as appropriately coloured bars.



**Fig. 21** Electricity price associated with equivalent financial properties with respect to the default supply chain: break-even hydrogen price ( ); net present value (x); payback period (+). FCEV filling cases, pale blue; fertiliser manufacturing cases, grey. Payback periods that did not have enough data to model are not shown in this figure.

While BEHP tells a large part of the financial story, it falls short in many places. The NPV data in Figure 20 shows the maximum NPV and slope for the linear 25-year NPV function. The most apparent result is that there are only two maximum NPV values that fail to reach profitability, suggesting that most electrolyser business cases can be very lucrative if coupled to a blend of dedicated VRE and LDE. Unsurprisingly, the cases with no economic viability are the usual suspects, supply chains **22** and **34**. These also have the lowest NPV depreciation rates of any supply chain other than the methyl formate variants. The highest NPV depreciation rates are shown by supply chains **38** and **40**. These are variants of liquid hydrogen supply chains that require over 500 MWh of electricity per day to liquefy the hydrogen produced through water electrolysis. The default supply chain sets the purchase price of electricity at 0.07 USD kWh<sup>-1</sup>, and if this price is reduced, it would lead to economic benefits towards the original OPEX as well. As a result, these supply chains have highly favourable economics with minimum BEHPs below 2.00 USD kg<sup>-1</sup> and very positive maximum NPVs. If implemented, this pair of supply chains would likely require the purchase of electricity at different prices throughout the day to power the liquefier, which may warrant the optimization of purchasing strategies in these cases. For the sake of simplicity, HBAT assumes a consistent average electricity price throughout



the entire lifetime of the business; therefore, readers should be aware the liquid hydrogen supply chains analysed in this study

will require electricity purchased at higher prices compared to other supply chains, due to the lack of consumption flexibility.

Although other properties such as the  $C_{TO}$  and IPM also have linear relationships with the electricity price, they do not provide any new information for this analysis. In contrast, the relationship between the payback period and electricity price is highly informative due to its correlation to the  $C_{TO}$  and EBITDA. Five data points were used to determine the best correlation function because the payback period is not linear. This function was found to be a power function, with a coefficient of determination of 0.9998. The minimum payback period is represented by the Y-intercept, but since this analysis used only two data points, the minimum payback period was determined by simulating all electrolyser supply chains at 0.00 USD kWh<sup>-1</sup> providing the third data point. These data were used to obtain estimated power functions for each supply chain. Figure S5 illustrates that even at prices of 0.04 USD kWh<sup>-1</sup>, the payback periods for all electrolyser supply chains were reduced. The power functions were extrapolated to determine the electricity price that would result in payback periods equivalent to those in the default scenarios. A similar extrapolation was performed for the linear BEHP and 25-year NPV functions, and the results are shown in Figure 21. It should be noted that the equivalent PBP price is greater than the equivalent BEHP and NPV prices. This pattern is due to the synergy between a dramatic reduction in TOC while lightly increasing OPEX. This Figure provides prospective businesses with valuable information to help determine which financial properties are most critical for their operations with the ultimate goal of making a more informed decision regarding the implementation of either the 10-hour dedicated strategy or the 23-hour smoothed strategy.

### 3.6 Cost-reduction analysis

Of the scenarios described above, the default 64 were repeated using a variable Annual Scaling Cost Reduction (ASCR) rate. This rate is shown in Equations 25 and 27 as %R<sub>2</sub>. The default rate is set to 5%, which describes the reduction in cost to increase production capacity by a certain extent. This is rationalised by factors such as R&D, process optimization, scaling optimization, and synergistic purchasing contracts. The 64 supplemental

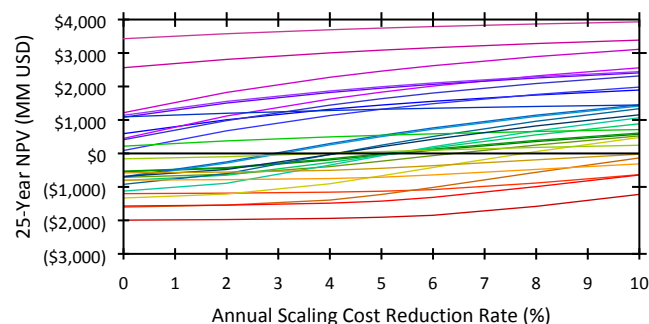


**Fig. 22** Net present value scaling functions for all 32 FCEV-filling supply chains. Data were collected at ASCR rates of 0%, 2%, 4%, 5%, 6%, 8%, and 10%. The legend indicating which coloured line corresponds to each supply chain is shown in Figure S7.

scenarios show theoretical benefits to achieving higher ASCR rates and provide insight on which supply chains benefit the most from reinvestment and scaling optimization.

$$B_{R\&D} = \frac{\Delta NPV}{ASCR_{OP}} \cdot \frac{\%D \cdot (1 + \%D)^{25}}{(1 + \%D)^{25} - 1}$$

For each business case, seven data points were collected spanning a range of 0 to 10%. Each data point includes the 25-year NPV, payback period, maximum profit margin, and EBITDA. Of these data, the 25-year NPV provided the most meaningful trends. Once the NPV gain is annualised using Equation 37, the annual R&D budget that can be allocated per percentage point in reduced cost for each business case. Risk is associated with how much cost reduction must be achieved to reach optimal profitability. Business cases that cannot reach profitability despite ASCR rates as high as 10% are labelled by the negative NPV border. High risk is defined as an ASCR rate of 10%, medium risk is between 4% and 6%, and low risk is defined as 2%. Fertiliser manufacturing cases shown in pale blue, FCEV filling shown in grey. Supply chain 54, 58, and 62 do not have FCEV data due to negative initial profitability. Label colours correspond to line colours in Figure 22.

Figure 23 shows the maximum R&D budget of each supply chain, along with the associated risk. This risk is defined proportionally to the optimal ASCR rate; the greater the optimal ASCR, the more dependent the business is on R&D. All 32 pairs of supply chains show greater R&D benefit in the FCEV-filling variant, with exception of the non-profitable. The figure shows that there are several front-runners in the technology that be used as reference points for existing production technologies. The remaining four scenarios involve formic acid (scenarios 8, 20, and 36) and ammonia (scenario 28) storage methods. These scenarios collectively have high economic potential due to the low operating cost of formic acid and ammonia storage. If the capital investment required for scaling can be reduced by R&D, the economics may be improved further.

distinguish supply chains with the highest R&D ceiling. As long as the desired ASCR rate is achieved using less annual spending than the R&D budget, the net benefit is an increase in NPV. Figure 22 shows that the FCEV-filling NPV functions are highly variable and unpredictable. To determine the optimal ASCR rate for each supply chain, it is necessary to identify the rate that provides the greatest marginal benefit. In other words, which ASCR rate provides the largest increase in NPV per percentage point of the ASCR. The table of optimal rates can be found in Table S4 of the supplemental information.

The fertiliser manufacturing NPV scaling function counterpart (Figure S7) shows less dependency on the ASCR rate. This effect is caused by the low growth ceiling of the fertiliser demand function. The result of this is visualised in the R&D budget chart in Figure 23. The chart shows the maximum R&D budget of each supply chain, along with the associated risk. This risk is defined proportionally to the optimal ASCR rate; the greater the optimal ASCR, the more dependent the business is on R&D. All 32 pairs of supply chains show greater R&D benefit in the FCEV-filling variant, with exception of the non-profitable. The figure shows that there are several front-runners in the technology

Definitions	
$B_{R\&D}$	Maximum annual R&D budget
$\Delta NPV$	Gain in 25-year net present value
$ASCR_{OP}$	Optimal annual scaling cost reduction rate
$\%D$	Annual discount rate (8%)

be used as reference points for existing production technologies. The remaining four scenarios involve formic acid (scenarios 8, 20, and 36) and ammonia (scenario 28) storage methods. These scenarios collectively have high economic potential due to the low operating cost of formic acid and ammonia storage. If the capital investment required for scaling can be reduced by R&D, the economics may be improved further.

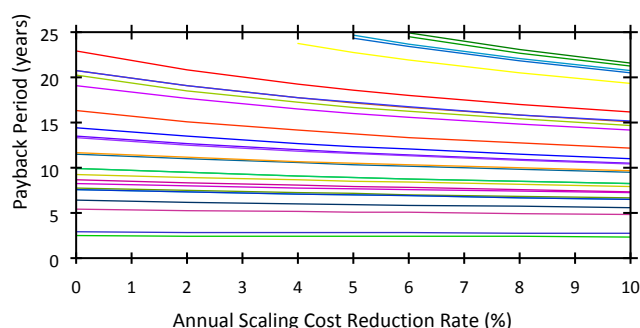
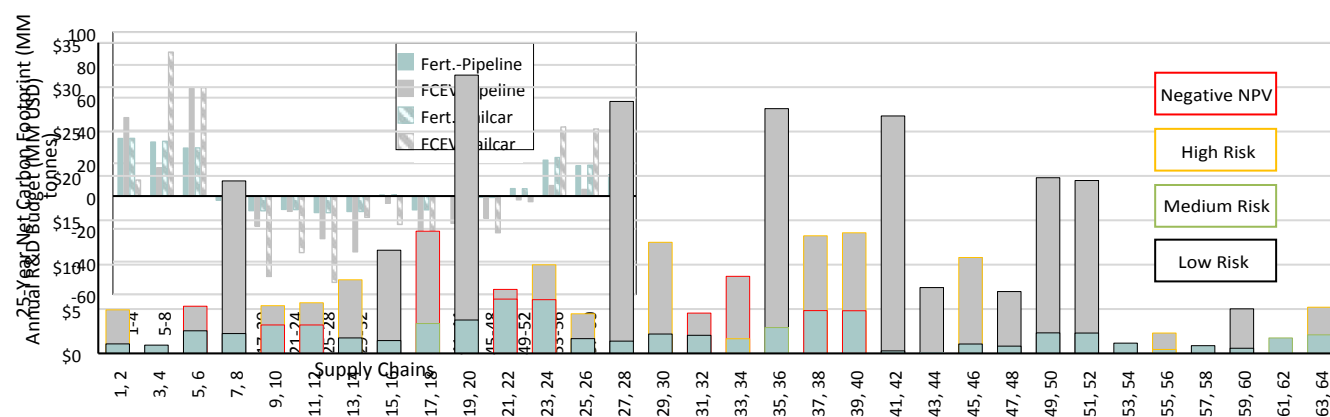


Fig. 25 Payback period scaling functions for the fertiliser manufacturing supply chains. The colours of each supply chain correspond to the legend in Figure S7 and match Figure 22, 23, and 24. Only supply chains with two or more payback periods that reach below 25 years are plotted in this chart.



Of the four non-SMR supply chains, only supply chain 8 has a lower R&D benefit compared to the top three SMR supply chains. These SMR supply chains have a high R&D benefit because of their specialised transportation technologies. Supply chain 42 sends gaseous hydrogen by pipeline across 824 km to supply FCEV filling stations, and supply chains 50 and 52 liquify their hydrogen before sending them by truck and railcar, respectively. The high capital investment of the pipeline and liquefier coupled to the low operating costs allow these business cases to benefit from R&D when scaling up. Supply chain 8 harbours a biomass gasification step that uses formic acid as an LOHC to send its hydrogen by railcar. Due to biomass contributing to nearly 60% of the operating cost, this business case does not have the same scale of benefits seen by the others previously mentioned. Nonetheless, it is still noteworthy in the figure due to its favourable balance between investment cost and initial profitability. Contrastingly, many of the business cases with less R&D benefit, such as supply chains 6 and 34, have high initial investment costs, resulting in low initial profit and slow scaleup making them less favourable for R&D. For some supply chains, such as supply chain 60, variable operating costs are too high despite having high initial profitability, making R&D efforts less effective.

ASCR displays an inverse relationship with payback period, typically in reverse order of the 25-year NPV as shown in Figure 24 and 25. Interestingly, except in a rare singular case, the payback period functions of each end-use do not overlap. Supply chain 8, which has a higher profitability index, crosses supply chain 44 and nearly reaches supply chain 28. The PI of each default business case correlates well with the payback period at an ASCR rate of 10%. Using Equations 38 and 39, linear regressions result in correlation coefficients of 0.996 and 0.992 for fertiliser and FCEV end-uses respectively. Furthermore, the FCEV coefficient can increase up to 0.997 excluding one outlier. The plots are shown in Figure S8.

$$(38) \quad A = -0.182C + 1.63$$

$$(39) \quad B = -49.91C + 141.6$$

$$\text{where } A = (PB)^{0.1769}, B = (PB)^{1.725}, C = \ln(PI)$$

This strong correlation between ASCR rates and payback period, confirms that high ASCR rates facilitate development of business cases with large initial investments, given that profit

margins are large enough to grow production proportionally with demand. For example, supply chain 20 reflects this concept with a  $C_{TO}$  of nearly one billion USD, but with an acceptable initial profit margin of 14.4%. The NPV of the business case can tolerate an annual R&D budget of 31.4 MM USD and still achieve a maximum payback period of 24.75 years as long as an ASCR rate of at least 1.9% is achieved.

### 3.7 Environmental impact

Until now, the economic viability of each business case was the only focus of the analysis. Here, the results from the previous sections are compared with the environmental impact of a given scenario. The environmental impact considers the variable carbon dioxide emissions, methane emissions, and nitrogen and sulphur oxide emissions. As discussed in Section 2.7, ANL's GREET is used for all emissions data. For further information on these calculations, we advise readers to refer to that section.

Decarbonising the energy industry is the primary goal of this analysis. This strategy targets the carbon emissions that are most accessible and malleable, those being the transportation emissions and existing hydrogen-producing industries, such as ammonia manufacturing. Due to these different applications,

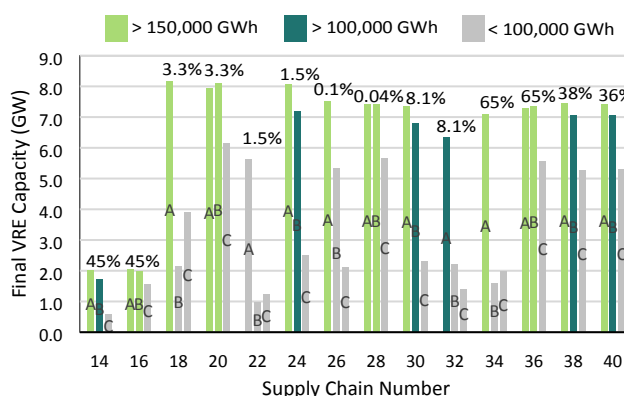


**Fig. 27** Renewable power production capacity after 25 years of expansion. Supply chains shown are FCEV filling scenarios that produce some quantity of renewable energy. Bar colours correspond with the total energy output of the proposed plant. Supply chains are grouped into the top 3 producing scenarios: A as the greatest and C as the third greatest. The groups are labelled with the minimum fuel cell efficiency necessary to produce electricity with less carbon emissions than the U.S. average, 0.855 lb kWh<sup>-1</sup>.

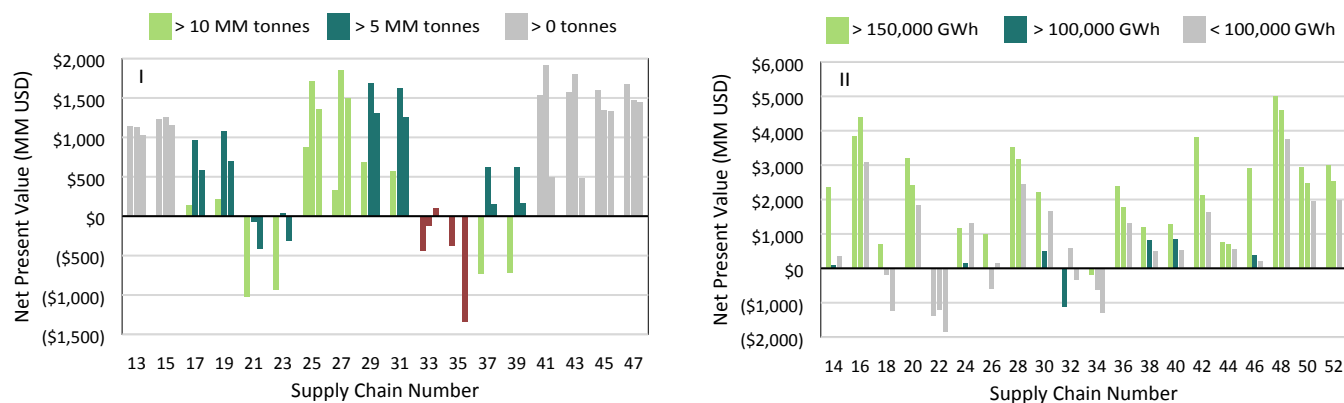


**Fig. 28** Net present value of the top three performing scenarios for each supply chain. Chart I shows fertiliser scenarios, ranked by total reduction in carbon emissions. Chart II shows FCEV-filling scenarios, ranked by total hydrogen energy output. A, B, and C labels are not shown here but the labelling still applies to each respective rank as explained in Figure 27.

each end-use modelled in this analysis will be compared to the existing *next best* option. For the FCEV-filling scenarios, the next best option is other zero-emission vehicles such as plug-in electric vehicles. The emissions of these vehicles depend on the emissions of the electricity source used to power them. The aggregate of all utility scale power plants in 2021 resulted in 1.65 billion metric tonnes of carbon dioxide emissions.<sup>50</sup> Using the total net electricity generation, the proportion is calculated to 388 g of CO<sub>2</sub> per kWh. This is used as the baseline for all FCEV-filling scenarios. The next best option for fertiliser manufacturing is the existing steam methane reforming process. The actual carbon footprint of the SMR process has been widely studied and reported to be anywhere between 8 and 11 kg of CO<sub>2</sub> per kg of hydrogen due to variations in the heating, compression, and purification efficiencies.<sup>51</sup> To eliminate variability, we assume all heat is provided by renewable electricity and ensure efficiency assumptions are consistent for every scenario. This results in a carbon footprint between 7.8 and 12.4 kg of CO<sub>2</sub> per kg of hydrogen depending on the storage and transportation technologies. To ensure conservative and fair conclusions, all fertiliser scenarios are compared to their corresponding pipeline or railcar SMR scenarios, to maintain consistency with original comparisons. Figure 26 shows the accumulated 25-year net carbon footprint of each default supply chain, relative to their respective reference. This result makes it evident that biomass gasification (supply chains 1 thru 12) is not an effective source of energy as it produces significantly more carbon dioxide emissions than their reference scenarios. Carbon monoxide purchasing (supply chains 53 thru 64) also has significant environmental drawbacks as these scenarios have been shown to emit only marginally less carbon dioxide than that of biomass gasification, but still greater than their references. Carbon monoxide purchasing may only be considered environmentally friendly if it was sourced from removing carbon monoxide from a waste stream that would otherwise contribute the same amount to carbon emissions; however, care should be taken to prevent increasing the demand for fossil fuel-derived carbon monoxide. For these reasons, these supply chains will not be studied in this environmental analysis.

The demand for hydrogen in FCEV-filling applications is predicted to grow at an exponential rate – as exemplified in

Section 2.4. This rate is large enough that it does not limit the growth rate of FCEV-filling business cases. Instead, the business' profit is what governs the scale-up rate. Consequently, the business' success can be measured by the total energy supplied by the hydrogen over the course of its lifetime. Figure 27 shows this by plotting the renewable power production capacity after 25 years for three of each FCEV-filling supply chain, ranked by the total energy output of the hydrogen product. The data shown in this section includes all scenarios that do not modify major assumptions. Changes to variables such as ASCR rate, discount rate, and feedstock price are not included because these scenarios cannot be compared one to one with other supply chains. The results show that all VRE-producing supply chains except supply chains 22 and 32 can reach a total energy output of 150,000 GWh. Many supply chains have only one scenario with specific conditions that lead to a successful business case. Apart from supply chain 16, all but supply chains use the 100,000 kg day<sup>-1</sup> case as the highest producing scenario. The economies-of-scale principle suggests that FCEV-filling business cases can benefit greatly from starting at a greater production capacity, as demonstrated by the magnitude of the positive NPV values in Figure 28-II compared to 28-I.

The NPV charts depicted in Figure 28 show the economic viability of the three best performing scenarios of each supply chain. Fertiliser manufacturing supply chains have relatively low

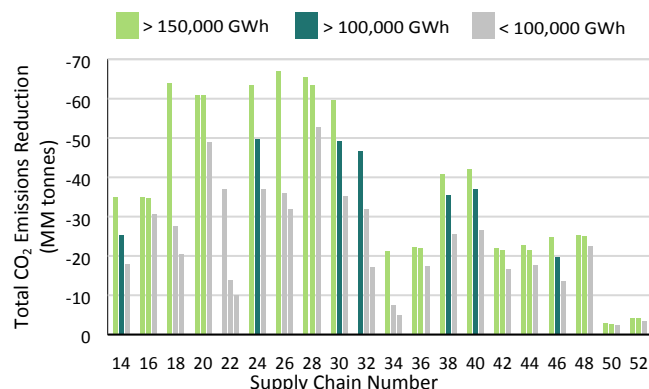


**Fig. 29** Total reduction in carbon dioxide emissions, relative to the respective reference. The three scenarios in each group are ranked by total hydrogen output, according to the colour scheme above. A, B, and C labels are not shown here but the labelling still applies to each respective rank as explained in Figure 27.

sales ceilings, so performance is determined by the total reduction in carbon dioxide emissions compared to their reference scenarios. One pattern that is immediately recognizable is that most electrolyser supply chains have a top-performing scenario that is less profitable, followed by two scenarios that have slightly worse emissions results. This is due to the 100,000 kg day<sup>-1</sup> scenario outperforming every other variation in scaling and VRE production. The two scenarios that typically follow this use the optimised utilisation strategy discussed in Section 3.4. They have significantly greater profitability but depend on LDE availability and cost assumptions that may not be realistic for the lifetime of the business. Nevertheless, the pattern shows that both strategies are viable, and perhaps the optimal solution is to use a combination of both during different regimes in the business' timeline.

The total energy output ranking used in Figure 28-II can also be applied to the total reduction in CO<sub>2</sub> emissions, shown in Figure 29. This chart is impactful because it weighs the scale of the production plant equally with the net carbon footprint. The supply chains with the greatest effect on global carbon emissions are **18, 20, 24, 26, 28** and **30**. They all have at least one scenario that achieves a positive NPV, but supply chains **20, 24, 28,** and **30** have two scenarios with NPVs greater than one billion USD. The top scenarios associated with these belong to the 100,000 kg day<sup>-1</sup> group and are among the best performing scenarios modelled in this analysis. Supply chains **20, 24, 28,** and **30** are a [CO<sub>2</sub> electrolysis] - [formic acid] - [railcar] business case,

**Table 4** Environmental spill effects caused by a 30-minute leak at high production.

	H <sub>2</sub>	CH <sub>4</sub>	CH <sub>3</sub> OH	HCOOCH <sub>3</sub>	HCOOH	NH <sub>3</sub>
M.T. Released	20.8 t	82.9 t	166 t*	207 t*	476 t	117 t
Longevity	10 y	12 y	28 h	48 h	14 h	N/A
Effect Type	Indirect GH	GH	Aquatic Toxicity	Aquatic Toxicity	Aquatic Toxicity	Aquatic Toxicity
Effect	20x GWP	30x GWP	15.4 g L <sup>-1</sup>	120 mg L <sup>-1</sup>	130 mg L <sup>-1</sup>	3.4 mg L <sup>-1</sup>
Effect Scale	417 t	2487 t	22 m <sup>a</sup>	120 m <sup>a</sup>	154 m <sup>a</sup>	326 m <sup>a</sup>

\*A spill to the scale suggested in this analysis would likely result in a fire due to flash points below room temperature; <sup>a</sup>Side length L of the cubic effect:  $V = L^3$

1. Yellow columns indicate a greenhouse effect; the scale is reported as an equivalent emission of CO<sub>2</sub> in metric tonnes by scaling the global warming potency (GWP)<sup>52, 53</sup>; GWP<sub>50</sub> and GWP<sub>100</sub> is used for H<sub>2</sub> and CH<sub>4</sub>, respectively.

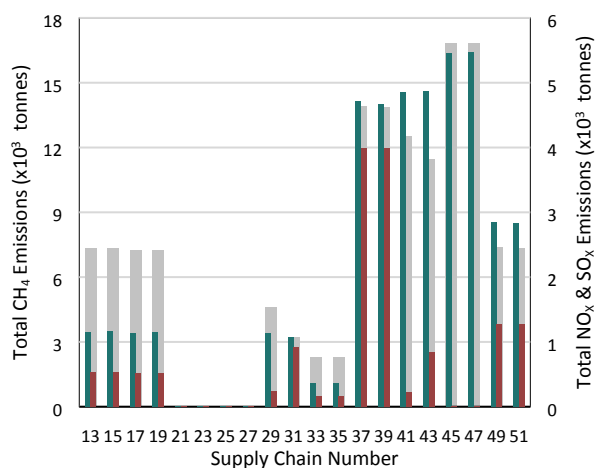
2. Blue columns indicate a toxic effect to aquatic ecosystems represented by the LC<sub>50</sub> for freshwater fish; the scale is reported as the height of a cube representing the total volume of water that is poisoned<sup>54-57</sup>

a [CO<sub>2</sub> electrolysis] - [methanol] - [railcar] business case, a [N<sub>2</sub> reduction] - [ammonia] - [railcar] business case, and a [water

electrolysis] - [compressed gas] - [pipeline] business case respectively. These four top scenarios achieve excellent reductions in carbon emissions and are able to generate profitable businesses, but there is a missing cost that HBAT is not able to model: environmental damage due to an unexpected spill. Historically, when accumulating and transporting large amounts of commodity chemicals, accidental spills occur at some point during the lifetime of the technology. If an unexpected spill is considered inevitable, then the damage to the environment caused by the spill must be considered prior to building the infrastructure. Table 3 shows the environmental effects of each of the hydrogen storage mediums used in the best-performing scenarios. The size of the spill is proportional to the hydrogen content by weight, scaled to the size of a 30-minute leak producing 1,000 metric tonnes day<sup>-1</sup> H<sub>2</sub>.

Ammonia is the most severely toxic for aquatic ecosystems, resulting in an LC<sub>50</sub> of just 3.4 mg L<sup>-1</sup>. Ammonia's lifetime in the environment is also difficult to predict because it depends on how quickly it can oxidise to its nitrate form, though this process is not much better. Oxidation of ammonia depletes oxygen from the surrounding water, creating long lasting effects that can permanently damage the ecosystem. Methyl formate and formic acid have similar, mild toxicities, at 120 and 130 mg L<sup>-1</sup> respectively. The major difference between them is the lifetime of these chemicals in the environment: methyl formate decomposes over 48 hours, however, it is very volatile and could ignite without warning, whereas formic acid will slowly decompose to carbon monoxide or oxidise to aqueous carbon dioxide over 14 hours. Methanol is much less toxic at an LC<sub>50</sub> of 15.4 g L<sup>-1</sup>. A methanol spill would only create a toxic aquatic environment for a 22 m tall cube, compared to 120 m, 154 m, and 326 m tall cube for methyl formate, formic acid, and ammonia respectively.

Unlike the liquid carriers, a hydrogen or methane gas leak would cause a cumulative greenhouse effect in the atmosphere rather than a short-term toxic effect. Methane has long been known to cause severe, but short-lived warming effects. Hydrogen does not directly cause a greenhouse effect, causing many to believe hydrogen emissions are inert. However, recent studies from Ocko and Hamburg<sup>52</sup> have shown that hydrogen reduces reactive oxidisers in the troposphere such as ·OH and O<sub>2</sub>. The depletion of these reactive species limits the troposphere's ability to degrade atmospheric methane and increases tropospheric ozone, both of which lead to further warming. Additionally, the by-product water increases moisture in the stratosphere, decreasing the amount of atmospheric heat radiated into space. Hydrogen's instantaneous warming potency is more than twice that of methane and more than 200 times that of carbon dioxide by mass. Since carbon dioxide's warming effects persist for nearly 100 years, it is difficult to accurately compare short-lived gases like hydrogen and methane. The U.S. Environmental Protection Agency estimates that methane's total warming potency is greater than 25 times that of carbon dioxide, so the effect scale in Table 3 is reported as the equivalent carbon dioxide emissions in metric tonnes. Hydrogen is even shorter lived than methane, but due to the



various indirect greenhouse effects, the global warming potency of hydrogen is estimated to be 20 times greater than carbon dioxide after 50 years of effects from a pulse of emissions. The 417-tonne effect caused by the hydrogen leak may appear to be substantial, but a renewable water electrolysis plant such as supply chain 30 would redeem the warming effect after only 51 minutes of production. (Equation S3) On the other hand, the methane leak would take more than 13 hours to redeem, assuming only renewable electricity is used to power the SMR plant. When viewed from the perspective of production time, an SMR plant cannot leak more than 3.6% of its methane feed without completely dissolving its slight

**Fig. 30** 25-year cumulative methane,  $\text{NO}_x$ , and  $\text{SO}_x$  emissions for fertiliser manufacturing scenarios (A) and FCEV filling scenarios (B). Grey, dark blue, and dark red bars represent methane,  $\text{NO}_x$ , and  $\text{SO}_x$  emissions, respectively.

environmental benefit from the renewable electricity. (Equation S4) The water electrolysis supply chain can leak up to 37% of its hydrogen and still enjoy a net benefit to the environment.

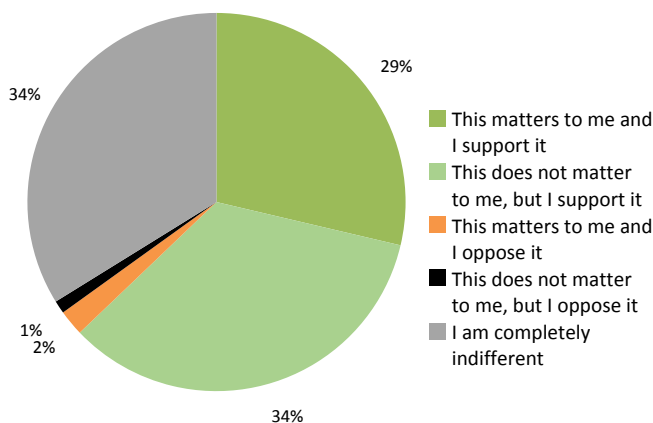
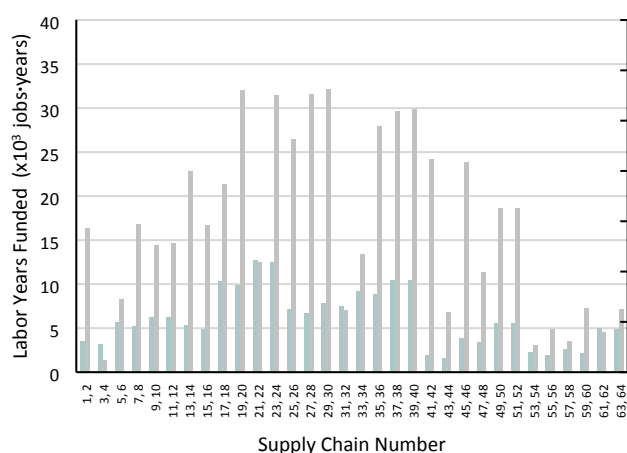


**Fig. 31** One-year jobs created for each default supply chain, accumulated over the 25-year life of the business. Fertiliser manufacturing (pale blue); FCEV filling (grey).

Global warming potency is the popular term to discuss when studying emissions, but other hazardous compounds such as nitrogen and sulfur oxides can contribute to the deterioration of environmental and respiratory health.  $\text{SO}_x$  and  $\text{NO}_x$  both result in environmental acidification and can create fine hazardous particles that can cause asthma and chronic bronchitis.<sup>58</sup>  $\text{NO}_x$  even contributes to the greenhouse effect by increasing the ozone concentration in the troposphere.<sup>59</sup> GREET gives estimates of these emitters for popular processes, but for more novel technologies such as ammonia dehydrogenation and methanol carbonylation, data does not yet exist. Therefore these numbers should be understood as floors for actual values, and should only be used to compare technologies within this report. Figure 30A and 30B show these emissions data for fertiliser manufacturing and FCEV filling supply chains respectively. Due to the nature of high-temperature steam reforming, the SMR supply chains have the greatest emissions of these damaging compounds. It is important to understand

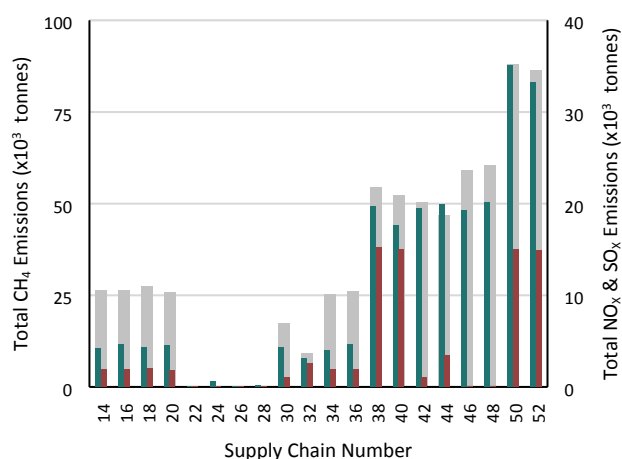


that supply chains **13** through **40** are electrolyser business cases. If these carriers are to be produced in other ways, such as Haber-Bosch for ammonia or SMR for methanol, the emissions data will completely change. Supply chain **38** and **40**

are both liquid hydrogen supply chains, so the apparent increase in emissions is due to the liquifier's process.

### 3.8 Societal impact

Though a flourishing hydrogen economy will create the benefit of a sustainable energy market, an additional benefit is a resilient self-sustaining labour market for skilled and non-skilled workers. The public buy-in for continued investment in sustainable energy technologies must be secured, and labour predictions such as the data shown in Figure 31 will facilitate that discussion. The number of jobs are calculated by using the monthly budget for maintenance material accumulated over the 25-year lifespan of the business and dividing it by \$120,000,



a typical median salary for a chemical manufacturer. This provides a good estimate on how many jobs are created because of the high labour costs of maintenance budgets. The FCEV-filling supply chains show the result of the growth available to this end-use, creating more jobs than most fertiliser supply chains by a factor of two or three. The electrolysis numbers (supply chains **13** thru **40**) are all fairly large because of the relatively high levelised cost of an electrolyser. This high cost requires significant maintenance and replacements, creating the demand for labour; supply chains **20**, **24**, **28**, and **30** all have superior labour numbers because of their large initial capital investments. Not shown here are the overhead labour and labour from supplemental budgets such as the R&D budgets mentioned in Section 3.6. These businesses also create the demand for highly-skilled labour in these markets, but salaries are quite dispersed and it is difficult to predict how they scale with production.

One of the most ideal locations to start developing the hydrogen economy is coastal Texas, USA for its proximity to industry and large populations that could support a growing FCEV market. As part of the Hydrogen Business Case Prize Competition sponsored by the U.S. Department of Energy, a poll was sent to 272 Chambers County residents to query their opinion on renewable energy and hydrogen. Seven other counties within the United States were also polled – these results can be seen in the supplementary information.

Interestingly, most counties show a similar proportion of indifferent voters and mildly supporting voters. In the Chambers County poll, 92 voted “I am completely indifferent” and 93 voted “This does not matter to me, but I support it”. This shows that the majority of people are not aware of how renewable energy and hydrogen can benefit them, so informing the public could pay dividends when trying to expand the FCEV and renewable electricity markets.

## 4 Summary and Conclusions

A renewable energy economy is the only option for sustained industrial expansion. Despite progress in cost reduction, availability, manufacturing, and efficiency, renewable energy supplied only 12.6% of the world's energy demand in 2022.<sup>60</sup> This slow growth is due in large part to the low capacity-utilization of most renewable energy generators. Hydrogen and liquid organic hydrogen carriers (LOHC's) provide a unique solution to this problem by enabling economies of scale to drive levelised costs of delivery much lower than current U.S. DOE estimates. Many techno-economic assessments of specific hydrogen technologies exist,<sup>61-68</sup> however, there are none that evaluate numerous variations of the supply chain using consistent and comparable assumptions. The Hydrogen Business Appraisal Tool (HBAT) consolidates many financial models for various hydrogen production, storage, and distribution methods. For the first time, a techno-economic analysis that provides economic, environmental, and societal analyses for the entire hydrogen supply chain is reported. Key investigations include efficient production capacities for each supply chain combination, optimal reinvestment strategies, and the economic effect of continued investment in R&D for technology efficiency and longevity.

In this analysis, 64 supply chains for producing and delivering hydrogen were studied using HBAT. Many variations of these supply chains were investigated by modifying financial parameters such as equipment depreciation rates, investment rates, initial production scale, etc. When evaluating business scenarios for expanding the hydrogen economy, it is important not to lose sight of the true goal: a sustainable and scalable market for green energy. Many production methods were evaluated in this report, such as wood biomass gasification and steam methane reforming, but the only ones capable of providing truly low-carbon hydrogen are the electrolyser production methods supplied with renewable electricity. Counter-intuitively, pine wood biomass gasification produces more carbon dioxide by weight than even steam methane reforming due to its high carbon content, making it unsuitable for utility scale power generation. Other rapidly growing biomass, such as microbial biomass, may be a solution, but they

**Fig. 32** Pie chart visualizing 272 Chambers County, Texas residents' responses to the question, “If U.S. Department of Energy plans to build a hydrogen powerplant for the expansion of renewable energy near Chambers County, what is your stance?” Polling was conducted using online community polls to maximise responses and will have bias towards residents who are online more often. All poll data from eight U.S. counties shown in supplementary data spreadsheet.

were not considered in this report due to unascertained economics.

The 64 supply chains were composed of six production pathways, seven storage mediums, three transportation methods, and two end-uses. In general, the fertiliser manufacturing end-use created business cases with the lowest initial investment costs because the transport distances were much smaller. Additionally, in the special case of nitrogen reduction, the product ammonia does not need to be dehydrogenated to supply the customer, reducing need for more equipment. Out of the transportation methods, railcar, truck, and pipeline, the railcar variant had greater economic viability in every case except when using the compressed hydrogen storage medium. This is the case because railcars and trucks have a volume and weight carrying capacity. Compressed hydrogen weighs so little that a tube-trailer truck and railcar can only hold 180 kg and 454 kg respectively. This is improved dramatically when liquefied, increasing the carrying capacity by more than twenty-fold, however, the cost of the cryogenic containers and liquefaction electricity tend to outweigh the benefits. The pipeline is compressed hydrogen's most efficient transportation method; supply chains such as the water electrolysis **29** and **30** are very economical despite their simplicity. The compressed hydrogen supply chains are well-rounded business cases, but they are outclassed by others when specific needs are desired. Methanol is generally the least viable hydrogen storage medium because of its high production and dehydrogenation investment cost. Though the transport cost is low, similar to ammonia, the need for complex production and dehydrogenation equipment diminishes the benefits. Methyl formate is the most interesting case because of its indirect storage potential. Methyl formate contains four hydrogen atoms per molecule, but its thermodynamics promote dehydrogenation of two water molecules per methyl formate molecule. This allows the business to transport two molecules of hydrogen directly and two molecules of hydrogen indirectly, leading to the highest volumetric hydrogen capacity of any medium at 131.9 kg H<sub>2</sub> m<sup>-3</sup>. The best methyl formate supply chain, **16**, takes advantage of this and becomes one of the highest earning supply chains. When considering carbon emissions, N<sub>2</sub> reduction, water electrolysis, and CO<sub>2</sub> to formic acid or methanol electrolysis produce the greatest net reduction in atmospheric carbon over 25 years. Out of these, supply chains **20** and **28** have the greatest balance of economic viability and emissions reduction.

Figure 7 labels each supply chain number with its respective technologies. Despite criticism for relying on narrow conclusions derived from levelised cost analyses,<sup>69</sup> this report evaluated the levelised cost of hydrogen (LCOH) for all supply chains used in Section 3.1. An SMR supply chain, **41**, has the lowest LCOH of all supply chains at 2.28 USD kg<sup>-1</sup>, while a nitrogen reduction supply chain, **27**, had the lowest electrolyser LCOH at 3.26 USD kg<sup>-1</sup>. Both **41** and **27** are fertiliser manufacturing supply chains because of the small distances required, but a methyl formate FCEV-filling supply chain, **16**, closely follows at 4.11 USD kg<sup>-1</sup>. This is an example of the trend

seen in Fig. 9 where all FCEV-filling supply chains have greater LCOHs than their fertiliser counterpart. Two groups separate themselves by their cost sensitivity to change in end-use: the scalable group has small differences in LCOH, such as the liquefier supply chains, while the economy group has large differences, such as the pipeline supply chains. The economy group tends to have low initial capital costs, leading to less depreciation and a lower LCOH. This benefit doesn't translate to the FCEV-filling end-use though, so high operating costs cause the LCOH to be higher than the scalable group. Therefore, the economy group is most optimally used in fertiliser manufacturing supply chains while the scalable group is most optimally used in FCEV-filling supply chains.

A levelised cost analysis is a useful tool to determine which technologies have the greatest potential to create low-cost products. However, one major flaw is that it assumes the technology does not improve over the course of its lifetime. Studying the break-even cost of a technology at a designated point in time results in much more accurate data that can be compared with other technologies and assumptions. In Section 3.3 and 3.5, the break-even hydrogen price (BEHP) was studied for all supply chains using various feedstock and energy prices. Figure 17 shows the electrolyser supply chains that have the opportunity of reaching delivered prices below 2.00 USD kg<sup>-1</sup> H<sub>2</sub>, namely, supply chains **19**, **20**, **25**, **27**, **28**, **29**, **30**, **31**, **38**, and **40**. Many of those have caveats, such as purchasing very low-cost, dispatch-constrained electricity (LDE) to supplement the supply for the electrolysers during 23 hours of the day rather than the default 10 hours with the solar arrays alone. Two supply chains, **25** and **27**, were able to achieve a BEHP of 2.00 USD kg<sup>-1</sup> by purchasing LDE at a reasonable price of 0.026 and 0.029 USD kWh<sup>-1</sup>, respectively. The non-renewable supply chains were also able to reach the same target BEHP, however like the electrolysers, both biomass gasification and CO purchasing supply chains depended on unrealistically low feedstock prices. SMR supply chains already currently provide hydrogen for less than 2.00 USD kg<sup>-1</sup>, nevertheless it is important to see the direct comparison of these supply chains using the HBAT assumption profile.

Water, carbon dioxide, and nitrogen are used as feedstocks for the electrolyser supply chains, each with its own advantages and disadvantages. Water electrolysis scenarios excelled when pipelines could be used to transport short distances. Carbon dioxide electrolysis scenarios excelled when the rail system can be taken advantage of to send LOHC's to as many consumers as possible. Lastly, nitrogen reduction scenarios excelled when supplying to fertiliser manufacturing customers since the dehydrogenation step could be avoided and investment costs minimised. During the environmental impact analysis, it was found that nitrogen reduction supply chains had the greatest risk of environmental damage, despite low carbon emissions. Storing and transporting ammonia in large quantities could be devastating to an ecosystem if a spill is inevitable – even a 30-minute leak at high production results in 34.5 million tonnes of toxic water. Shipping vessels can contain nearly three orders of magnitude more than the amount used in these calculations.

Nevertheless, the nitrogen reduction scenarios are among the most profitable, with two of the top-5 highest NPV scenarios belonging to N<sub>2</sub> reduction. Unsurprisingly, the FCEV-filling scenarios had much higher NPVs (23 of the top-25) because of the growth allowed, but fertiliser manufacturing scenarios typically had lower BEHPs.

The top-4 NPV scenarios all belong to 100,000 kg day<sup>-1</sup>, railcar, and FCEV-filling supply chains. This shows the significant economic benefit of starting at larger scales and highlights the opportunity of the U.S. rail system. The top NPV scenario belongs to the CO<sub>2</sub> electrolysis to methyl formate supply chain **16**, scenario 328: achieving a PBP of 6.9 years, a BEHP of 2.35 USD kg<sup>-1</sup>, and an NPV of 4,400 MM USD. The drawback of this scenario is the high carbon footprint – at 5.87 kg of CO<sub>2</sub> emissions per kg of H<sub>2</sub>, it doesn't reach the low carbon threshold and must be labelled as grey hydrogen. Renewably sourced methanol would solve this problem, but it was not included in the scope of this analysis. Uninterestingly, the second-best NPV scenario is a 40% reinvestment scenario of the same supply chain as 328. Ignoring duplicate supply chains, the next best NPV scenario is the 100,000 kg day<sup>-1</sup>, N<sub>2</sub> reduction to ammonia supply chain **28**, scenario 340: achieving a PBP of 13.16 years, a BEHP of 1.80 USD kg<sup>-1</sup>, and an NPV of 3,500 MM USD. The only major drawback to this scenario is ammonia's inherent toxicity; scaled up enough to supply a state's FCEV-filling market, 12 hours of ammonia inventory could toxify 16 miles of the Mississippi River. As the fourth highest NPV scenario, the 100,000 kg day<sup>-1</sup> CO<sub>2</sub> electrolysis to formic acid supply chain **20**, scenario 332, falls slightly behind due to the smaller hydrogen storage capacity: achieving a PBP of 13.58 years, a BEHP of 2.13 USD kg<sup>-1</sup>, and an NPV of 3,200 MM USD. These three business cases are close in NPV and could all be viable in the coming hydrogen economy, but there are clear leaders in some areas. Scenario 328 has the largest NPV because it combines renewable carbon monoxide with cheap NG-sourced methanol to make methyl formate, selling four times as much hydrogen per molecule of carbon monoxide than other CO<sub>2</sub> electrolysis scenarios. Scenario 340 has the lowest BEHP of any FCEV-filling scenario because ammonia has the highest inherent hydrogen density of any molecule in this study; it only needs to run seven railcars at a time to ship 100,000 kg day<sup>-1</sup> of hydrogen, while scenario 332 needs to run twenty-four for the same revenue. Scenario 332 is a balanced scenario that has great economics, impact on carbon emissions reduction, and labour numbers, while reducing the negative impact of a major spill if or when it occurs. Supply chains **20** and **28** are both leaders in electrolyser longevity benefit (Figure 16), R&D potential (Figure 23), carbon emissions reduction (Figure 29), and societal impact (Figure 31).

Global energy markets and hydrogen seem destined to unite. The path to that future is still somewhat unclear, but evidently those technologies that will lead this important economic change already exist.

## Author Contributions

N.A.V.: Conceptualization, Data Curation, Funding Acquisition, Formal Analysis, Investigation, Methodology, Project Administration, Writing – Original Draft, Review & Editing; M.K.: Data Curation, Funding Acquisition, Investigation, Writing – Original Draft, Review & Editing; C. D. A. V.: Conceptualization, Data Curation, Funding Acquisition, Formal Analysis, Investigation, Software, Visualization; D. F. A.: Conceptualization, Data Curation, Funding Acquisition, Investigation, Methodology, Validation, Visualization; J. T. E.: Data Curation, Funding Acquisition, Investigation, Visualization.

## Conflicts of interest

N. A. V. is a founder of a company, Solargonic LLC, that aims to commercialise liquid hydrogen carriers.

## Acknowledgements

This work was accomplished with the financial support from the Hydrogen Business Case Competition hosted by the National Renewable Energy Laboratory and the Hydrogen and Fuel Cell Technologies Office. The authors are also very grateful for the support from Dr. Robert Currier from the Los Alamos National Laboratory and Dr. Mariya Koleva from the National Renewable Energy Laboratory for their consultation.

## Notes and references

1. International Energy Agency, *Net Zero by 2050 – A Roadmap for the Global Energy Sector*, Paris, 2021.
2. More than half of new U.S. electric-generating capacity in 2023 will be solar, <https://www.eia.gov/todayinenergy/detail.php?id=55419#>, (accessed May 2023).
3. B. Frew, B. Sergi, P. Denholm, W. Cole, N. Gates, D. Levie and R. Margolis, *Joule*, 2021, **5**, 1143-1167.
4. Frequently Asked Questions (FAQs) – U.S. utility-scale electricity generation by source, amount, and share of total in 2022, <https://www.eia.gov/tools/faqs/faq.php?id=427&t=3#:~:text=In%202022%2C%20about%204%2C243%20billion,facilities%20in%20the%20United%20States.&text=About%2060%25%20of%20this%20electricity,%2C%20petroleum%2C%20and%20other%20gases>, (accessed June 2023).
5. M. S. Zantye, A. Gandhi, Y. Wang, S. P. Vudata, D. Bhattacharyya and M. M. F. Hasan, *Energy & Environmental Science*, 2022, **15**, 4119-4136.
6. A. Blakers, M. Stocks, B. Lu and C. Cheng, *Progress in Energy*, 2021, **3**, 022003.
7. C. Diyoke, M. Aneke, M. Wang and C. Wu, *RSC Advances*, 2018, **8**, 22004-22022.
8. C. A. Hunter, M. M. Penev, E. P. Reznicek, J. Eichman, N. Rustagi and S. F. Baldwin, *Joule*, 2021, **5**, 2077-2101.
9. R. Gibrat, presented in part at the Hydrogen energy; Proceedings of the Hydrogen Economy Miami Energy Conference, Miami Beach, Florida, 1974.
10. A. Susmozas, D. Iribarren and J. Dufour, *Resources*, 2015, **4**, 398-411.

11. R. S. El-Emam, H. Ozcan and C. Zamfirescu, *Journal of Cleaner Production*, 2020, **262**, 121424.
12. A. Midilli, H. Kucuk, M. E. Topal, U. Akbulut and I. Dincer, *International Journal of Hydrogen Energy*, 2021, **46**, 25385-25412.
13. S. Masoudi Soltani, A. Lahiri, H. Bahzad, P. Clough, M. Gorbounov and Y. Yan, *Carbon Capture Science & Technology*, 2021, **1**, 100003.
14. Cemvita's Successful Field Test Demonstrates Gold Hydrogen Production in Situ, <https://www.cemvita.com/news/cemvitas-successful-field-test-demonstrates-gold-hydrogen-tm-production-in-situ>, (accessed June 2023).
15. T. Zhang, J. Uratani, Y. Huang, L. Xu, S. Griffiths and Y. Ding, *Renewable and Sustainable Energy Reviews*, 2023, **176**, 113204.
16. H. Shui, R. Ge, D. Zou, S. Ren, Z. Li, J. Yan, Z. Lei and Z. Wang, *Fuel*, 2022, **323**, 124382.
17. N. Lazouski, M. Chung, K. Williams, M. L. Gala and K. Manthiram, *Nature Catalysis*, 2020, **3**, 463-469.
18. International Energy Agency, *Global Hydrogen Review 2022*, Paris, 2022.
19. International Renewable Energy Agency, *Global hydrogen trade to meet the 1.5°C climate goal: Part I – Trade outlook for 2050 and way forward*, Abu Dhabi, 2022.
20. U.S. Department of Energy, Hydrogen and Fuel Cell Technologies Office – Hydrogen Shot, <https://www.energy.gov/eere/fuelcells/hydrogen-shot>, (accessed July 2022).
21. N. Alfonso Vargas, C. D. Alfonso Vargas, D. F. Alfonso, M. Kim, J. T. Evans, *Hydrogen Business Appraisal Tool*, <https://www.solargenic.com/hbat>, (accessed August 2023).
22. National Renewable Energy Laboratory, *H2A: Hydrogen Analysis Production Models*, <https://www.nrel.gov/hydrogen/h2a-production-models.html>, (accessed March 2022).
23. D. Feldman, V. Ramasamy, R. Fu, A. Ramdas, J. Desai and R. Margolis, *U.S. Solar Photovoltaic System and Energy Storage Cost Benchmark: Q1 2020*, Golden, Colorado, 2020.
24. J. Lee, W. Lee, K. H. Ryu, J. Park, H. Lee, J. H. Lee and K. T. Park, *Green Chemistry*, 2021, **23**, 2397-2410.
25. J. R. Gomez, J. Baca and F. Garzon, *International Journal of Hydrogen Energy*, 2020, **45**, 721-737.
26. J. Cha, Y. Park, B. Brigljević, B. Lee, D. Lim, T. Lee, H. Jeong, Y. Kim, H. Sohn, H. Mikulčić, K. M. Lee, D. H. Nam, K. B. Lee, H. Lim, C. W. Yoon and Y. S. Jo, *Renewable and Sustainable Energy Reviews*, 2021, **152**, 111562.
27. M. Byun, B. Lee, H. Lee, S. Jung, H. Ji and H. Lim, *International Journal of Hydrogen Energy*, 2020, **45**, 24146-24158.
28. B. Labbaf, M. Tabatabaei, E. Mostafavi, M. Tijani and N. Mahinpey, *Process Safety and Environmental Protection*, 2021, **148**, 1346-1356.
29. Y. K. Salkuyeh, B. A. Saville and H. L. MacLean, *International Journal of Hydrogen Energy*, 2018, **43**, 9514-9528.
30. A. Kramer, *Advanced Gasifier and Water Gas Shift Technologies for Low Cost Coal Conversion to High Hydrogen Syngas*, Des Plains, Illinois, 2016.
31. D.-Y. Lee, A. Elgowainy and Q. Dai, *Applied Energy*, 2018, **217**, 467-479.
32. M. Ruth, P. Jadun, N. Gilroy, E. Connelly, R. Boardman, A. J. Simon, A. Elgowainy and J. Zuboy, *The Technical and Economic Potential of the H2@Scale Concept within the United States*, Golden, CO, 2020.
33. E. Rezaei and S. Dzurik, *Chemical Engineering Research and Design*, 2019, **144**, 354-369.
34. U.S. Department of the Treasury, *Treasury Department and Internal Revenue Service Release Final Rule on Section 45Q Credit Regulations*, <https://home.treasury.gov/news/press-releases/sm1227>, (accessed October 2023).
35. J.-E. Bae, S. Wilailak, J.-H. Yang, D.-Y. Yun, U. Zahid and C.-J. Lee, *Energy Conversion and Management*, 2021, **231**, 113835.
36. U.S. Department of Energy, *2022 Annual Merit Review Awards: Hydrogen Technologies – Storage and Infrastructure*, [https://www.hydrogen.energy.gov/annual-review/annual\\_review22\\_awards.html](https://www.hydrogen.energy.gov/annual-review/annual_review22_awards.html), (accessed July 2022).
37. N. Alfonso, T. Williams, R. Currier, A. Chavez, V. Do, US Pat., 0332574, 2022.
38. T. Williams, R. P. Currier, *HyMARC Seedling: Hydrogen Release from Concentrated Media with Reusable Catalysts*, [https://www.hydrogen.energy.gov/docs/hydrogenprogramlibraries/pdfs/review22/st216\\_williams\\_2022\\_p-pdf.pdf](https://www.hydrogen.energy.gov/docs/hydrogenprogramlibraries/pdfs/review22/st216_williams_2022_p-pdf.pdf)
39. L. Lu, Z. Li, X. Chen, H. Wang, S. Dai, X. Pan, Z. J. Ren and J. Gu, *Joule*, 2020, **4**, 2149-2161.
40. M. P. Kohn, M. J. Castaldi and R. J. Farrauto, *Applied Catalysis B: Environmental*, 2014, **144**, 353-361.
41. S. J. Yoon, Y.-C. Choi, Y.-I. Son, S.-H. Lee and J.-G. Lee, *Bioresource Technology*, 2010, **101**, 1227-1232.
42. G. A. Olah, *Angewandte Chemie International Edition*, 2005, **44**, 2636-2639.
43. M. Nielsen, E. Alberico, W. Baumann, H.-J. Drexler, H. Junge, S. Gladiali and M. Beller, *Nature*, 2013, **495**, 85-89.
44. C. Smith, A. K. Hill and L. Torrente-Murciano, *Energy & Environmental Science*, 2020, **13**, 331-344.
45. M. Mintz, J. Gillette, J. Li, A. Elgowainy, M. Paster, M. Ringer and D. Brown, *Hydrogen Delivery Scenario Analysis Model for Hydrogen Distribution Options*, Lemont, Illinois, 2006.
46. U.S. Department of Transportation Federal Railroad Administration, *New Tank Car Standards for Crude Oil and Ethanol Rail Shipments*, Washington DC, 2016.
47. M. Wang, A. Elgowainy, U. Lee, A. Bafana, S. Banerjee, P. Benavides, P. Bobba, A. Burnham, H. Cai, U. Gracida-Alvarez, T. Hawkins, R. Iyer, J. Kelly, T. Kim, K. Kingsbury, H. Kwon, Y. Li, X. Liu, Z. Lu, L. Ou, N. Siddique, P. Sun, P. Vyawahare, O. Winjobi, M. Wu, H. Xu, E. Yoo, G. Zaimes and G. Zang, *Summary of Expansions and Updates in GREET® 2021*, Lemont, Illinois, 2021.
48. CertifHy, *CertifHy Scheme*, [https://www.certifhy.eu/wp-content/uploads/2022/06/CertifHy\\_Scheme-Documents\\_V2.0\\_2022-04-28\\_endorsed\\_CLEAN.pdf](https://www.certifhy.eu/wp-content/uploads/2022/06/CertifHy_Scheme-Documents_V2.0_2022-04-28_endorsed_CLEAN.pdf), (accessed February 2023).
49. M. Niermann, S. Drunert, M. Kaltschmitt, K. Bonhoff, *Energy & Environmental Science*, 2019, **12**, 290-307
50. U.S. Energy Information Administration, *Emissions by plant and by region*, <https://www.eia.gov/electricity/data/emissions>, (accessed February 2022).
51. P. Sun, B. Young, A. Elgowainy, Z. Lu, M. Wang, B. Morelli

- and T. Hawkins, *Environmental Science & Technology*, 2019, **53**, 7103-7113.
52. I. B. Ocko and S. P. Hamburg, *Atmos. Chem. Phys.*, 2022, **22**, 9349-9368.
53. P. Balcombe, J. F. Speirs, N. P. Brandon and A. D. Hawkes, *Environmental Science: Processes & Impacts*, 2018, **20**, 1323-1339.
54. Sigma-Aldrich, *Methanol Safety Data Sheet*, <https://www.sigmaaldrich.com/US/en/sds/sial/322415>, (accessed April 2023).
55. Sigma-Aldrich, *Methyl Formate Safety Data Sheet*, <https://www.sigmaaldrich.com/US/en/sds/ALDRICH/W519103>, (accessed April 2023).
56. Sigma-Aldrich, *Formic Acid Safety Data Sheet*, <https://www.sigmaaldrich.com/US/en/sds/sigald/f0507>, (accessed April 2023).
57. Sigma-Aldrich, *Ammonia Safety Data Sheet*, <https://www.sigmaaldrich.com/US/en/sds/aldrich/294993>, (accessed April 2023).
58. M. Kowalska, M. Skrzypek, M. Kowalski and J. Cyrus, *International Journal of Environmental Research and Public Health*, 2020, **17**, 754.
59. G. Lammel and H. Graßl, *Environmental Science and Pollution Research*, 1995, **2**, 40-45.
60. Our World in Data, *Energy Mix*, <https://ourworldindata.org/energy-mix>, (accessed March 2023).
61. A. W. Bartling, M. L. Stone, R. J. Hanes, A. Bhatt, Y. Zhang, M. J. Bidy, R. Davis, J. S. Kruger, N. E. Thornburg, J. S. Luterbacher, R. Rinaldi, J. S. M. Samec, B. F. Sels, Y. Román-Leshkov and G. T. Beckham, *Energy & Environmental Science*, 2021, **14**, 4147-4168.
62. R. Dickson, M. S. Akhtar, A. Abbas, E. D. Park and J. Liu, *Green Chemistry*, 2022, **24**, 8484-8493.
63. M. van der Spek, C. Banet, C. Bauer, P. Gabrielli, W. Goldthorpe, M. Mazzotti, S. T. Munkejord, N. A. Røkke, N. Shah, N. Sunny, D. Sutter, J. M. Trusler and M. Gazzani, *Energy & Environmental Science*, 2022, **15**, 1034-1077.
64. A. Poluzzi, G. Guandalini and M. C. Romano, *Sustainable Energy & Fuels*, 2022, **6**, 3830-3851.
65. M. Niermann, S. Drünert, M. Kaltschmitt and K. Bonhoff, *Energy & Environmental Science*, 2019, **12**, 290-307.
66. M. R. Shaner, H. A. Atwater, N. S. Lewis and E. W. McFarland, *Energy & Environmental Science*, 2016, **9**, 2354-2371.
67. T. Terlouw, C. Bauer, R. McKenna and M. Mazzotti, *Energy & Environmental Science*, 2022, **15**, 3583-3602.
68. C. E. Finke, H. F. Leandri, E. T. Karumb, D. Zheng, M. R. Hoffmann and N. A. Fromer, *Energy & Environmental Science*, 2021, **14**, 1517-1529.
69. E. Loth, C. Qin, J. G. Simpson and K. Dykes, *Advances in Applied Energy*, 2022, **8**, 100112.